

Modeling of Recent ElectricOIL Gain Recovery Data

Andrew D. Palla¹, David L. Carroll², and Joseph T. Verdeyen³
CU Aerospace, Champaign, IL 61820

and

Joe W. Zimmerman⁴, Brian S. Woodard⁴, Gabriel F. Benavides⁴, Michael T. Day⁴, and Wayne C. Solomon⁵
University of Illinois at Urbana-Champaign, Urbana, IL, 61801

Experiments and modeling have led to continued enhancements in the Electric Oxygen-Iodine Laser (ElectricOIL) system. This continuous wave (cw) laser operating on the 1315 nm transition of atomic iodine is pumped by the production of O₂(a) in a radio-frequency (RF) discharge in an O₂/He/NO gas mixture. New discharge geometries and increases in gain length, flow rates, discharge power, and resonator mode volume have improved the peak measured gain to 0.26% cm⁻¹ and the outcoupled laser power to 102 W. The BLAZE model has been used to perform end-to-end (discharge through laser resonator) simulations of the new system configuration to help guide this process. Results are in good agreement with data. Additional measurements of gain recovery downstream of an operating laser cavity for five cases of interest are presented and modeled. The deviation of the gain recovery data from calculations based on presently accepted theory is highlighted. Several potential mechanisms to explain this theory are presented and discussed.

I. Introduction

The electrically driven oxygen-iodine laser (ElectricOIL) that was first demonstrated by Carroll *et al.* [Carroll, 2004; Carroll, 2005] operates on the electronic transition of the iodine atom at 1315 nm, $I(^2P_{1/2}) \rightarrow I(^2P_{3/2})$ [denoted hereafter as I^* and I respectively]. The lasing state I^* is produced by near resonant energy transfer with the singlet oxygen metastable O₂(a¹Δ) [denoted hereafter as O₂(a)]. Since the first reporting of a viable electric discharge-driven oxygen-iodine laser system (also often referred to as EOIL or DOIL in the literature), there have been a number of other successful demonstrations of gain [Rawlins, 2005; Verdeyen, 2006; Hicks, 2007] and laser power [Verdeyen, 2006; Hicks, 2007; Bruzzese, 2009], as well as a recent demonstration of gain and lasing from an air-helium discharge [Woodard, 2008]. Computational modeling of the discharge and post-discharge kinetics [Stafford, 2005; 2006a-b; Palla, 2007a-b] has been an invaluable tool in ElectricOIL development, allowing analysis of the production of various discharge species [O₂(a¹Δ), O₂(b¹Σ), O atoms, and O₃] and determination of the influence of NO_x species on system kinetics. Ionin *et al.* [Ionin, 2007] and Heaven [Heaven, 2010] provide comprehensive topical reviews of discharge production of O₂(a) and various ElectricOIL studies. As of today, the highest gain in an ElectricOIL device reported to date was 0.26 % cm⁻¹, with an output power of 102 W [Carroll, 2010].

One of the significant remaining questions regarding the ElectricOIL system is: why is the amount of laser power extracted so much lower than the available power carried by the O₂(a)? For example, for the peak gain and power case we have a laser output power of 102 W for a flow that calculations indicate has approximately 540 W of power carried downstream by O₂(a). While the BLAZE model [Palla, 2006a-b; Palla, 2007a-b] has demonstrated good agreement with the experimental measurements for production of various discharge species and laser gain, Fabry-Perot laser simulations with the BLAZE model indicate that for this case we should be able to extract

¹ Senior Physicist, CU Aerospace, 2100 S. Oak St. – Ste 206, Champaign, IL 61820, Senior Member AIAA.

² Vice President / COO, CU Aerospace, 2100 S. Oak St. – Ste 206, Champaign, IL 61820, Associate Fellow AIAA.

³ Senior Scientist, CU Aerospace, 2100 S. Oak St. – Ste 206, Champaign, IL 61820.

⁴ Research Assistant, Univ. of Ill. at Urbana-Champaign, 104 S. Wright, Urbana, IL 61801, Student Member AIAA.

⁵ Professor Emeritus, Univ. of Ill. at Urbana-Champaign, 104 S. Wright, Urbana, IL 61801, Fellow AIAA.

approximately 230 W in laser power, yet we are only getting a little over 100 W. The two possible causes that seem the most likely suspects: (i) optical losses that dissipate power before it is outcoupled, and (ii) an unidentified chemical kinetic process that is somehow inhibiting (slowing) the power extraction process.

Carroll and Verdeyen [Carroll, 2009b] explored the possibility that Fraunhofer diffraction that occurs off the edges of the supersonic cavity (which effectively act as an aperture) could create a significant optical loss mechanism for the ElectricOIL experiments to date which have employed mirrors with very high reflectivity (typically > 0.9999). They made a conservative estimate that the expansion angle in recent experiments is $\sin\theta \approx \theta = \lambda/d = 1.315 \mu\text{m}/2.54 \text{ cm} = 5.2 \times 10^{-5}$ radians. They then estimated the amount of beam area from diffractive expansion that could be clipped by the apertures; this estimate comes out to be a loss of approximately 0.00056 per restricting aperture for the geometry studied. While this number seems at first glance to be very small, when one considers the number of passes the photons make through a high reflectivity resonator, then even small intracavity losses may have a significant effect. Carroll and Verdeyen concluded that a small diffractive loss would have a significant effect on ElectricOIL performance; this hypothesis was verified by Benavides *et al.* [Benavides, 2009].

Measurements of gain recovery downstream of an operating laser cavity were performed by Zimmerman *et al.* [Zimmerman, 2009]. Modeling of these experiments showed that reducing the forward and backward pumping rates by an effective factor of approximately 4 to simulate a competing mechanism results in the computational modeling matching the experimental gain recovery measurements, and in improved agreement between the measured and modeled laser power extraction. Note that Zimmerman *et al.* [2009] are not suggesting that the established pumping rates are in error, only that there is an additional competing process that is occurring in the ElectricOIL system kinetics potentially due to additional species not present in classic COIL. These experiments suggested that a larger volume resonator that extends further downstream in the flow direction may be able to extract more power from the ElectricOIL gain medium; this was verified by Woodard *et al.* [Woodard, 2010]. In this paper a baseline case simulation of the current best gain and power case is presented. Additional measurements of gain recovery downstream of an operating laser cavity for five cases of interest are presented and modeled. The deviation of the gain recovery data from calculations based on presently accepted theory is highlighted. Several potential mechanisms to explain this theory are presented and discussed.

II. BLAZE-IV Model

CU Aerospace developed BLAZE-IV [Palla, 2007a-b; Palla, 2006a-b], a multi-physics simulation software package, for physical system analysis. The model was developed using the C++ programming language using modern data abstraction and encapsulation techniques to simplify extensions of the model, at the most basic level, to any problem of interest. BLAZE-IV includes fluid-dynamic, electrodynamic, thermodynamic, plasma-kinetic/kinetic, optical, and elastic solid mechanical modules and is capable of solving multi-dimensional transient and steady-state cell-centered finite-volume problems using both structured and unstructured grids in addition to temporal and spatial marching problems. The model is capable of generating structured rectilinear grids, unstructured grids comprised of triangles (2D) or tetrahedrons (3D) computed using an adaptive Delaunay tessellation scheme, and unstructured grids comprised of n-polygons (2D) or hexahedrons (3D). Additional elements have been added to automate parametric studies by systematic variation of specified parameters. The model has been successfully deployed in a number of widely varied engineering research programs. The research described herein utilized the 1-D spatial marching-mixing model component of the BLAZE-IV model.

The calculations presented in this paper assume a kinetic set comprised of the 52 species: e^- , He, $\text{He}(^1\text{S})$, He^+ , $\text{O}_2(^3\text{X})$, $\text{O}_2(^3\text{X},v=1)$, $\text{O}_2(^3\text{X},v=2)$, $\text{O}_2(^3\text{X},v=3)$, $\text{O}_2(^3\text{X},v=4)$, $\text{O}_2(^3\text{X},v=5)$, $\text{O}_2(a^1\Delta)$, $\text{O}_2(a^1\Delta,v=1)$, $\text{O}_2(a^1\Delta,v=2)$, $\text{O}_2(a^1\Delta,v=3)$, $\text{O}_2(a^1\Delta,v=4)$, $\text{O}_2(a^1\Delta,v=5)$, $\text{O}_2(b^1\Sigma)$, $\text{O}_2(b^1\Sigma,v=1)$, $\text{O}_2(b^1\Sigma,v=2)$, $\text{O}_2(b^1\Sigma,v=3)$, $\text{O}_2(b^1\Sigma,v=4)$, $\text{O}_2(b^1\Sigma,v=5)$, O_2^- , O_2^+ , O, $\text{O}(^1\text{S})$, $\text{O}(^1\text{D})$, $\text{O}(3p^3\text{P})$, $\text{O}(3p^5\text{P})$, O^+ , O^- , O_3 , O_3^- , N_2 , I_2 , IO, INO, INO_2 , $\text{I}_2(v=20)$, $\text{I}_2(^3\Pi_{2U})$, $\text{I}_2(^3\Pi_{1U})$, $\text{I}_2(^3\Pi_{0+U})$, $\text{I}(^2\text{P}_{3/2})$, $\text{I}(^2\text{P}_{1/2})$, NO, NO^+ , $\text{NO}(v>0)$, NO_2 , NO_2^* , NO_2^- , NO_2^+ , and NO_3 . The calculations draw from the ElectricOIL reaction set presented in Appendix 1 (note that not all reactions were necessarily employed in the current study, e.g., nitrogen electrodynamics and vibrational disequilibrium processes are only used if there is significant nitrogen in the discharge).

III. Baseline Calculations

The peak power baseline case assumes a 3.5 kW, 24" discharge with inlet flow rates of $\text{O}_2:\text{He}:\text{NO} = 45:150:0.26$ mmol/s at 49 Torr and 300 K. The discharge is followed by a 2" axial flow length reduced cross-

sectional flow area cooling block that is modeled via specification of a thermal boundary layer thickness that is baselined to best match downstream gas temperature data. The modeled $I_2:He = 0.38:40$ mmol/s, 329 K iodine stream is injected at $M=0.5$ via 21 circular holes with a total cross-sectional area of 0.1412 cm^2 (the injected stream Mach Number is used to determine initial stream momentum and the injector count partially determines the surface area over which stream mixing interaction occurs). The modeled $N_2 = 300$ mmol/s at 79.15 K diluent stream is injected at $M=0.5$ via 42 circular holes with a total cross-sectional area of 0.444 cm^2 . The mixing streams flow into a geometric Mach 2.5 nozzle in which a supersonic boundary layer growth model is employed. The optical axis is located 8.36 cm downstream of the nozzle throat and the gain length is 3". The stable resonator (which is modeled as a Fabry-Perot resonator) is comprised of a pair of 4" diameter $R = 0.997$, $T = 0.00298$ mirrors. The calculated $O_2(a^1\Delta)$ and $O_2(b^1\Sigma)$ yields and gas temperature as a function of axial location for the non-lasing case are presented in Figure 1. The discharge exit $O_2(a^1\Delta)$ yield is predicted to be approximately 12.5% and increases slightly in the post-discharge region as the flow cools and the $O_2(b^1\Sigma)$ is partially converted to $O_2(a^1\Delta)$, Fig. 1. The gas temperature reaches nearly 600 K at the discharge exit but is cooled rapidly in the post-discharge cooling block and due to supersonic expansion, Fig. 1.

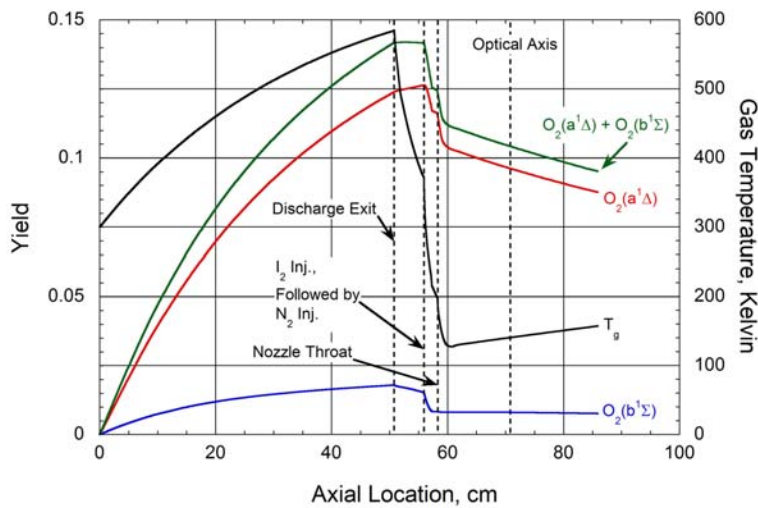


Fig 1. Baseline case calculated $O_2(a^1\Delta)$, $O_2(b^1\Sigma)$, and $O_2(a^1\Delta) + O_2(b^1\Sigma)$ yields and gas temperature as a function of axial location.

The predicted small signal gain is shown to be in good agreement with data in the resonator region, Fig. 2.

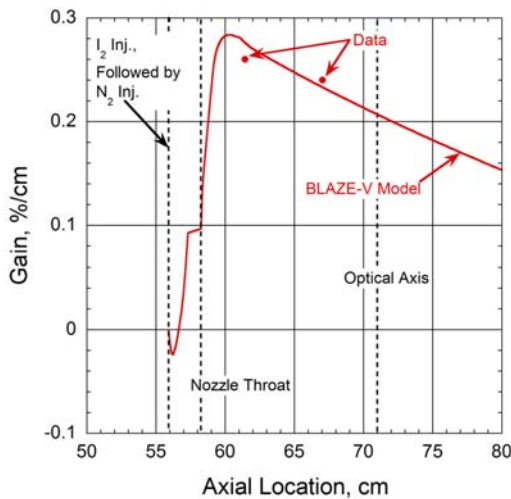


Fig 2. Baseline case calculated small signal gain compared to data as a function of axial location.

In the lasing case, Figure 3, the $O_2(a^1\Delta)$ power flux upstream of the resonator follows the same trends as the $O_2(a^1\Delta)$ yield in the non-lasing case with moderate losses occurring downstream of the iodine injection point. The peak $O_2(a^1\Delta) + O_2(b^1\Sigma)$ power flux is predicted to be near 650 W, of which approximately 230 W is extracted optically, Fig. 3.

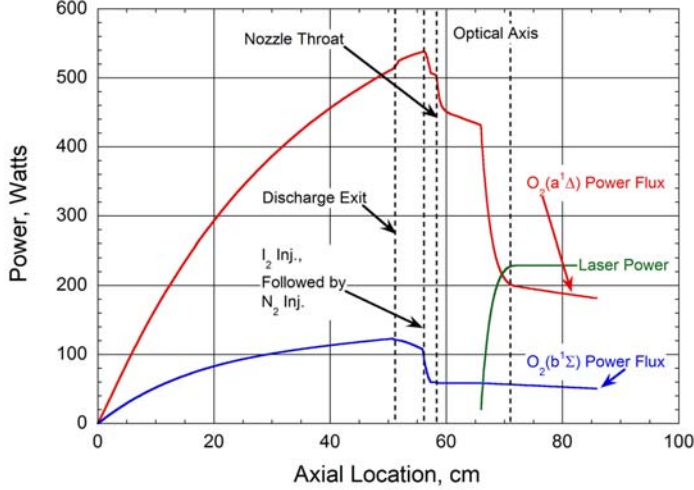


Fig 2. Baseline case calculated $O_2(a^1\Delta)$ and $O_2(b^1\Sigma)$, power fluxes and outcoupled laser power as a function of axial location.

Although specie concentrations, gas temperature, and gain are well modeled, the outcoupled laser power is significantly over-predicted (230 W versus 102 W).

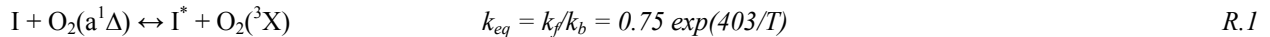
IV. Modeling of Gain Recovery Data

Previous data [Zimmerman, 2009] indicated that gain recovered to the equilibrium value downstream of a laser resonator slower than predicted by theory; with this mechanism possibly inhibiting laser power extraction, gain recovery was measured and subsequently modeled for five current cases of interest. Small signal gain and gain recovery downstream of a 1" diameter laser resonator were measured for a case similar to the peak gain and power case. Similar measurements were also taken for cases with varied I_2 and NO flow rates, and a case with a reduced resonator R_1R_2 value. The configurations used in the five cases are summarized in Table 1.

Case	I_2 Flow Rate, mmol/s	NO Flow Rate, mmol/s	R_1	R_2	Peak Gain, %/cm	Power, W
1	0.38	0.26	0.99997	0.99995	0.2165	9.64
2	0.30	0.054	0.99997	0.99995	0.1402	4.4
3	0.23	0	0.99997	0.99995	0.1097	0.2
4	0.36	1.2	0.99997	0.99995	0.0957	3.2
5	0.21	0.19	0.997	0.997	0.1256	29.2

Table 1. Gain recovery case configurations and measured peak gain and laser power.

The gain recovery rate (equivalently, the rate at which the gain achieves equilibrium with the flow and kinetics) is dependent upon the $O_2(a^1\Delta) \leftrightarrow I^*$ energy transfer reaction, R.1.



Research by Van Marter *et. al.* [Van Marter, 1998] has indicated a low-temperature backward rate constant defined by $k_b(150K) = (7.0 \pm 0.7) \times 10^{-12} \text{ cm}^3 \text{ s}^{-1} \text{ molec.}^{-1}$. In addition, research in [Van Marter, 1996] indicated a temperature dependence of $T^{0.5}$ provided good agreement with available data. Combining the temperature dependence with the low temperature backward rate data point, $k_f = 6.288 \times 10^{-12} \text{ T}^{1/2} \text{ cm}^3 \text{ s}^{-1} \text{ molec.}^{-1}$ and $k_b = 8.392 \times 10^{-12} \text{ T}^{1/2} \exp(-403/T) \text{ cm}^3 \text{ s}^{-1} \text{ molec.}^{-1}$ were determined.

While previous calculations have indicated that good agreement with gain recovery data may be achieved via approximation of the unidentified mechanism by reducing both k_f and k_b by an identical factor (note that reduction

by the same factor preserves the equilibrium constant), the gain recovery data was initially modeled using the standard rates presented above. Lasing and non-lasing simulations of each of the gain recovery experiment configurations listed in Table 1 were performed. Simulations of the gain recovery experiments using the standard rates for R.1 significantly over-predicted power extraction and therefore also likely significantly under-predicted the $O_2(a^1\Delta)$ yield at the resonator trailing edge. The under-predicted $O_2(a^1\Delta)$ yield at the resonator trailing edge makes a comparison of the predicted gain recovery rates using the standard reaction rates with data questionable. In order to eliminate this problem, an additional simulation of each gain recovery experiment was performed using the standard rates, but with the resonator mode width (in the flow direction) reduced to near zero while leaving the resonator trailing edge position fixed. In the resulting simulations, the gain saturates but only a small amount of power is extracted (as in the experiments), making direct model to experiment comparisons of gain recovery rate more meaningful.

Calculated gain in the case 1 non-lasing simulation is in good agreement with data while the lasing simulation equilibrium gain achieved several centimeters downstream of the resonator trailing edge is approximately half of the value indicated by data, Fig. 4. Note that equilibrium gain implies that the I^*/I ratio has reached a value such that R.1 is locally balanced. Again, this discrepancy between the calculated equilibrium gain value and data is likely the result of the significantly over-predicted power extraction using the standard rates, ~65 W vs. 9.6 W from data, Tables 1 and 2. The case 1 short mode width lasing simulation was in good agreement with laser power data, 9.4 W vs. 9.6 W, Tables 1 and 2, while the gain recovery rate downstream of the resonator trailing edge was significantly over-predicted, Fig. 4. A parametric study was performed in which the full mode width lasing simulation presented in Figure 4 was repeated with the forward and backward R.1 rates multiplied by a range of factors less than unity (again note that the same multiplier was applied to the forward and backward rates to preserve the equilibrium constant). A multiplier of 0.318 was determined to minimize the sum of the squares of the deviations between each gain recovery data point and the calculation for the case 1 configuration. Non-lasing and lasing simulations were performed using R.1 rates reduced by this factor and assuming the full resonator width. Lasing calculations using the reduced reaction rates were in good agreement with gain data as a function of distance from the resonator trailing edge, Fig. 5.

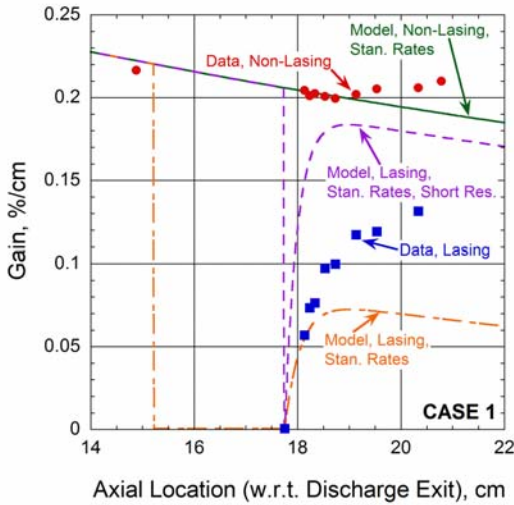


Fig 4. Gain recovery case 1 calculated gain assuming standard $O_2(a^1\Delta) \leftrightarrow I^*$ energy transfer rates as a function of system configuration and axial location compared to data as a function of axial location.

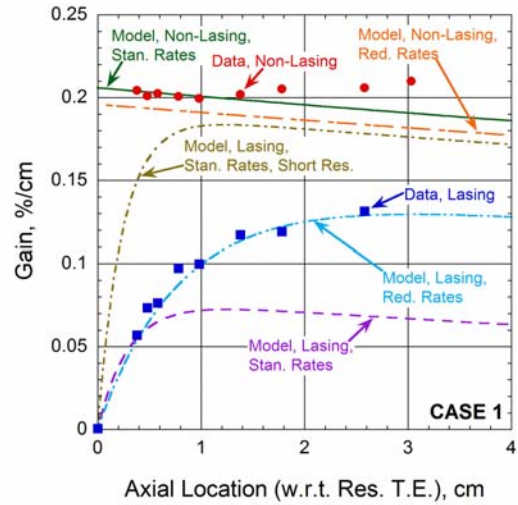


Fig 5. Gain recovery case 1 calculated gain assuming standard or best fit $O_2(a^1\Delta) \leftrightarrow I^*$ energy transfer rates as a function of system configuration and axial location compared to data as a function of axial location.

Case	$O_2(a^1\Delta) \leftrightarrow I^*$ Rate Reduction Factor	Power, W (Standard Rates)	Power, W (Standard Rates, Short Resonator)	Power, W (Reduced Rates)
1	0.318	65.07	9.36	32.64
2	0.314	46.38	6.17	21.18
3	0.564	42.87	5.17	28.79
4	0.307	53.23	4.21	20.53
5	0.305	69.36	7.51	27.63

Table 2. Gain recovery case configurations.

Gain recovery case 2, which has reduced I_2 (0.23 vs. 0.38 mmol/s) and NO (0.054 vs. 0.26 mmol/s) flow rates as compared to case 1, was modeled using a procedure identical to that used to model case 1. A reduction factor of 0.314 applied to R.1 was found to give best agreement with gain recovery data. The correlation of calculated results to data was similar to the correlation in case 1, Figs. 6 and 7.

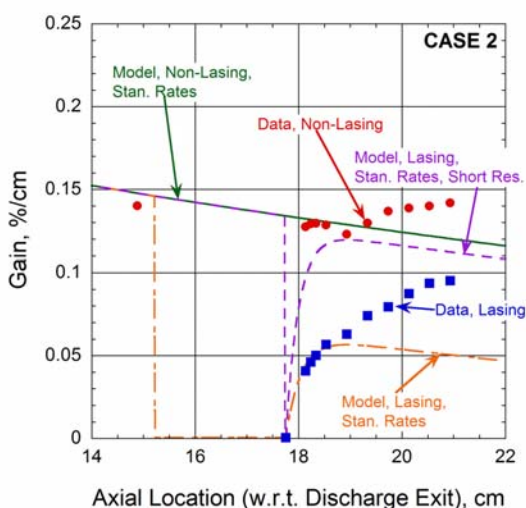


Fig 6. Gain recovery case 2 calculated gain assuming standard $O_2(a^1\Delta) \leftrightarrow I^*$ energy transfer rates as a function of system configuration and axial location compared to data as a function of axial location.

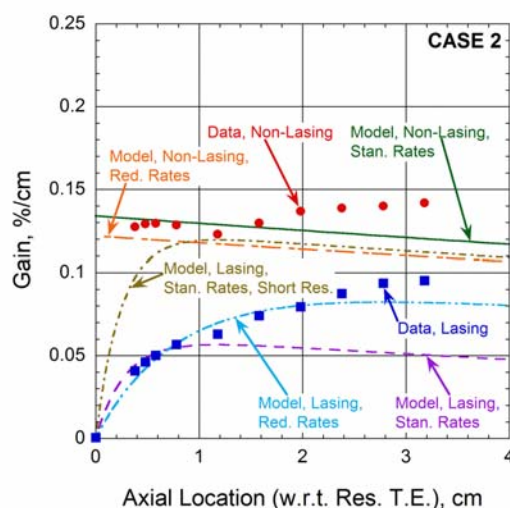


Fig 7. Gain recovery case 2 calculated gain assuming standard or best fit $O_2(a^1\Delta) \leftrightarrow I^*$ energy transfer rates as a function of system configuration and axial location compared to data as a function of axial location.

Gain recovery case 3, which has reduced I_2 (0.30 vs. 0.38 mmol/s) and NO (0 vs. 0.26 mmol/s) flow rates as compared to case 1, was modeled using a procedure identical to that used to model case 1. A reduction factor of 0.564 applied to R.1 was found to give best agreement with gain recovery data. The qualitative correlation of calculated results to data was similar to the correlation in case 1, Figs. 8 and 9. However, calculated results for case are significant in that the 0.564 R.1 reduction factor that gives best agreement with data is significantly different than the ~ 0.3 reduction factor that provided best agreement in all other cases presented in this study and in previous studies. This is also the only case to date without NO for which gain recovery data has been recorded.

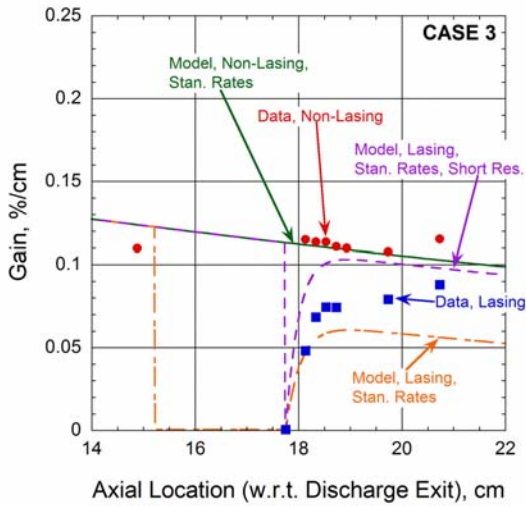


Fig 8. Gain recovery case 3 calculated gain assuming standard $O_2(a^1\Delta) \leftrightarrow I^*$ energy transfer rates as a function of system configuration and axial location compared to data as a function of axial location.

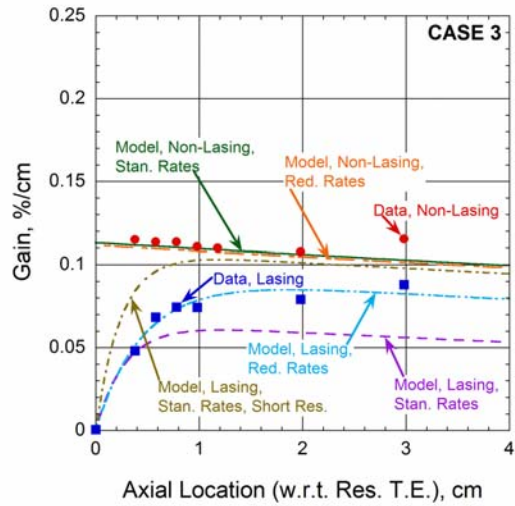


Fig 9. Gain recovery case 3 calculated gain assuming standard or best fit $O_2(a^1\Delta) \leftrightarrow I^*$ energy transfer rates as a function of system configuration and axial location compared to data as a function of axial location.

Gain recovery case 4, which has a similar I_2 (0.36 vs. 0.38 mmol/s) flow rate and a substantially increased NO (1.2 vs. 0.26 mmol/s) flow rate as compared to case 1, was modeled using a procedure identical to that used to model case 1. A reduction factor of 0.307 applied to R.1 was found to give best agreement with gain recovery data. The correlation of calculated results to data was similar to the correlation in case 1, Figs. 10 and 11.

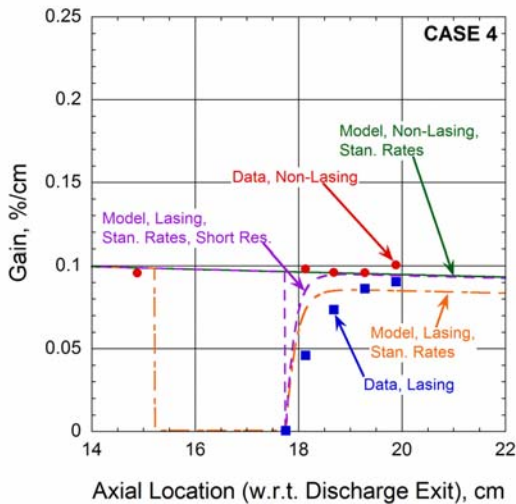


Fig 10. Gain recovery case 4 calculated gain assuming standard $O_2(a^1\Delta) \leftrightarrow I^*$ energy transfer rates as a function of system configuration and axial location compared to data as a function of axial location.

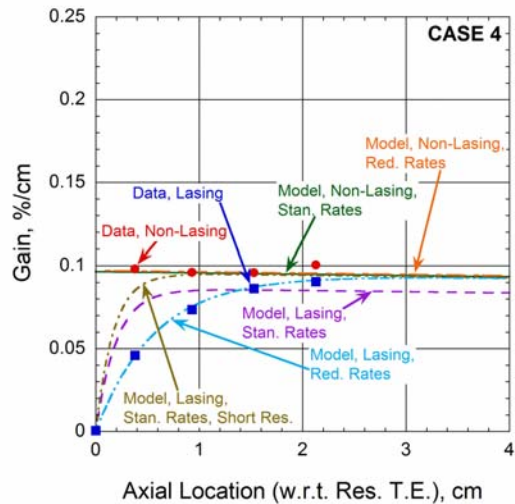


Fig 11. Gain recovery case 4 calculated gain assuming standard or best fit $O_2(a^1\Delta) \leftrightarrow I^*$ energy transfer rates as a function of system configuration and axial location compared to data as a function of axial location.

Gain recovery case 5, which has reduced I_2 (0.21 vs. 0.38 mmol/s) and NO (0.19 vs. 0.26 mmol/s) flow rates and a reduced resonator R_1R_2 (0.994 vs. 0.99992) value as compared to case 1, was modeled using a procedure identical to that used to model case 1. A reduction factor of 0.305 applied to R.1 was found to give best agreement with gain recovery data. The correlation of calculated results using standard R.1 rates to data was similar to the correlation in case 1, Figs. 12 and 13. However, the calculated equilibrium gain downstream of the resonator in the reduced R.1 rate lasing simulation was significantly less than data, likely as a result of over-predicted power

extraction or losses, Fig. 13. Therefore the chosen optimum reduction factor of 0.305 was the reduction factor that optimized the correlation of gain recovery curve shape to data after correcting for magnitude.

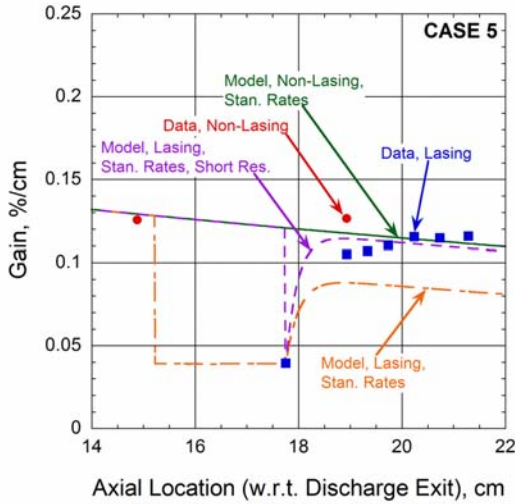


Fig 12. Gain recovery case 5 calculated gain assuming standard $O_2(a^1\Delta) \leftrightarrow I^*$ energy transfer rates as a function of system configuration and axial location compared to data as a function of axial location.

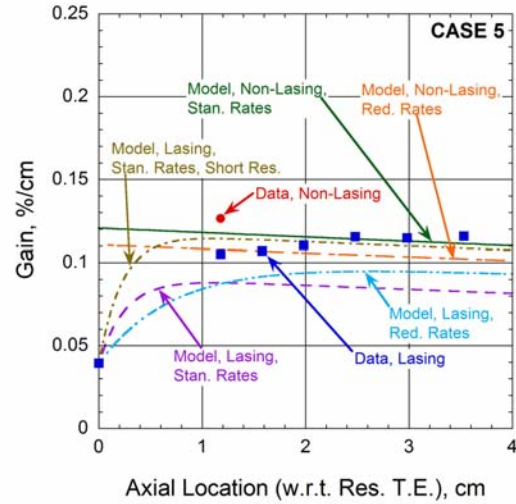


Fig 13. Gain recovery case 5 calculated gain assuming standard or best fit $O_2(a^1\Delta) \leftrightarrow I^*$ energy transfer rates as a function of system configuration and axial location compared to data as a function of axial location.

The optimum R.1 reduction factor determined for each gain recovery case and calculated powers using the standard rates with the standard and reduced width resonators and calculated powers using the reduced rates are summarized in Table 2. Calculated laser powers are compared graphically in Figure 14.

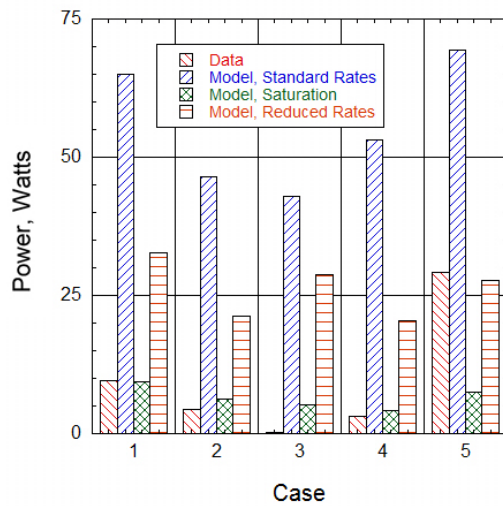


Fig 14. Gain recovery cases 1 to 5 calculated laser power as a function of $O_2(a^1\Delta) \leftrightarrow I^*$ energy transfer rates and system configuration compared to data.

The simulations of gain recovery cases 1-5 have indicated that good agreement with gain recovery downstream of an operating laser resonator may be achieved via simultaneous reduction of the R.1 forward and backward rate constants as an approximation of an unidentified mechanism. Calculations have indicated that a reduction factor of approximately 0.3 is optimum for all modeled cases except the case without NO. A reduction factor of approximately 0.56 is optimum for the case without NO. It is possible that a significant error in the predicted laser power extraction and kinetic losses upstream of the laser resonator in the modeling of the gain recovery case without NO might explain the significant difference in apparent gain recovery rate as compared to the remaining cases. However, the difference in apparent gain recovery rates is sufficient to suggest that it is likely to

be at least partially real. This result does not however, guarantee that the actual mechanism that is inhibiting gain recovery in the EOIL system is either directly or indirectly dependent on NO.

V. Potential Mechanisms

Multiple potential physical mechanisms are discussed herein to explain the trends observed in gain recovery downstream of an operating resonator. First, it was theorized that an optical or kinetic loss mechanism in the resonator region may be the cause of the discrepancy between gain recovery data and theory. These first two possibilities should be discussed simultaneously because an optical effect (e.g. diffraction) or a kinetic loss mechanism (e.g. an additional I^* quenching mechanism) would both result in a lower $O_2(a^1\Delta)$ yield at the resonator trailing edge than might otherwise be predicted from the gain or $O_2(a^1\Delta)$ yield upstream of the laser resonator and the laser power that was extracted. In other words, the amount of extracted laser power corresponds to a relatively small amount of $O_2(a^1\Delta)$ loss, and a diffractive and/or kinetic quenching loss would manifest itself as a further reduction in $O_2(a^1\Delta)$ that does not show up in the measured gain recovery. The reduced $O_2(a^1\Delta)$ yield at the resonator trailing edge would further result in an apparently reduced gain recovery rate. However, this category of potential effects may be immediately discounted as the *primary* mechanism inhibiting gain recovery in the cases described in this paper. Examining the calculations presented in the previous section, most cases with the standard R.1 rates and the short mode width resonator predicted laser powers reasonably close to data, Tables 1 and 2. However, taking case 1 as an example, when the full mode width resonator is modeled with the standard R.1 rates, the predicted laser power is significantly greater than data. The resulting reduction in predicted $O_2(a^1\Delta)$ yield at the resonator trailing edge is sufficient to reduce the gain recovery rate to match the rate indicated by data, Fig. 5. However, the reduced $O_2(a^1\Delta)$ yield at the resonator trailing edge also leads to an equilibrium gain downstream of the resonator trailing edge that is implausibly below data, Fig. 5. The implication is clear: if an optical or kinetic mechanism acted in the resonator region to reduce the $O_2(a^1\Delta)$ yield at the resonator trailing edge sufficiently to reduce the gain recovery rate to match data, the resulting downstream equilibrium gain would be significantly below data. Specifically, for case 1, an $O_2(a^1\Delta)$ yield of $\sim 5.2\%$ is required at the resonator trailing edge to match equilibrium gain data several centimeters downstream, but an $O_2(a^1\Delta)$ yield of $\sim 3.6\%$ is required to match the gain recovery slope using the standard R.1 rates. Obviously this is impossible. Therefore the mechanism inhibiting gain recovery in the cases described in this paper must be one that is predominantly lossless. Further evidence can be observed in case 4 and 5 data and calculations, where the lasing case gain data downstream of the resonator recovers to a value near to the predicted gain in the non-lasing cases, Figs. 11 and 13. If there were significant losses in the resonator region in the lasing case, the difference between lasing and non-lasing case gain would be much greater downstream of the resonator. It should also be noted that an additional unidentified iodine recombination or loss mechanism in the resonator region would also produce an effect similarly inconsistent with data: a reduced gain recovery rate to an equilibrium gain correspondingly below data.

A potential mechanism that may appear to meet the requirements for matching gain recovery data is a 3-body energy transfer process, R.2, acting in addition to R.1.



The quantum efficiency of R.2 is identical to that of R.1, so the lossless criterion as described above is met. To study the effects of this mechanism, an equation was derived to constrain the reaction rates for R.2 such that the axial rate of change of I^* (which correlates to the axial rate of change in gain) due to the sum of R.1 and R.2 is equal to the axial rate of change of I^* due to R.1 alone multiplied by a constant c .

$$\frac{k_{f1}[I][O_2(a)] - k_{b1}[I^*][O_2] + k_{f2}[I][O_2(a)][M] - k_{b2}[I^*][O_2][M]}{k_{f1}[I][O_2(a)] - k_{b1}[I^*][O_2]} = c \quad E.1$$

Equation 1 constrains the rates of R.2 to achieve a desired multiplicative change in the axial I^* concentration (and therefore gain) derivative. Equation 1 may be manipulated to specify the forward reaction rate for R.2, k_{f2} , given a specified equilibrium constant for R.2, k_{eq2} , via

$$k_{f2} = \frac{k_{eq2}(1-c)(k_{f1} - \eta k_{b1})}{[M](\eta - k_{eq2})}, \quad \eta = \frac{[I^*][O_2]}{[I][O_2(a)]} \quad E.2$$

where $[M]$ is the local concentration of the assumed third body specie, and η is the local ratio of the left hand to right hand reactant concentrations in R.1. At the trailing edge of the resonator in the reduced R.1 rate lasing simulation from the previous section, which we believe best predicts conditions at that location, the gas temperature is predicted to be 120.1 K which determines a $k_{eq1} \approx 21.5$, and η is predicted to be approximately 9.7. Given these values, E.2 implies that in order to match the initial gain recovery data slope, the equilibrium constant k_{eq2} cannot be more than $\sim 1/2$ of the equilibrium constant k_{eq1} , regardless of the choice of M , without indicating a meaningless, negative forward reaction rate, k_{f2} . This is due to the $(\eta - k_{eq2})$ denominator term, E.2.

Given the k_{eq2} constraint described above, gain recovery was modeled for the case 1 configuration assuming k_{eq2} values of 0.1, 0.2, 0.5, 1, 2 and 5. The forward reaction rate for R.2, k_{f2} , was determined for each k_{eq2} value using E.2, in order to match the initial case 1 gain recovery slope. Case 1 gain recovery data, and predicted gain recovery curves using the standard and reduced R.1 rates only are compared to the predicted gain recovery curves using the R.1/R.2 mechanism described above assuming each of the listed k_{eq2} values in Figure 15. The calculated results indicate that regardless of the choice of R.2 equilibrium constant, specification of the R.2 forward reaction rate such that the initial gain recovery slope is accurately modeled, causes the final equilibrium gain downstream of the resonator trailing edge to be significantly under-predicted, Fig. 15. Note that in these cases atomic oxygen was chosen as the third body specie M , but the results would be nearly identical for any choice of $[M]$ that does not vary significantly as a function of axial location in the gain recovery region. Calculations have indicated that the specification of R.2 rates such that the calculated initial gain recovery slope is consistent with data results in an equilibrium gain significantly below data, Fig. 15. Therefore, calculations were performed in which $k_{eq2} = k_{eq1}$ in an attempt to match the equilibrium gain predicted by R.1 alone (and indicated by data). Atomic oxygen was again used as the third body specie M , and a range of k_{f1} values were modeled, producing scenarios in which R.2 is dominant with respect to R.1, R.2 is on the order of R.1, and R.2 is insignificant with respect to R.1. As was expected, when R.2 is insignificant with respect to R.1, the standard R.1 rates results from the previous section are reproduced, Fig. 16. As the magnitude of R.2 is increased with respect to the fixed R.1 magnitude, the gain recovery slope increases, while the final equilibrium gain remains nearly constant, Fig. 17. Calculations indicate that if the R.2 rates are adjusted to accurately predict the gain recovery slope, Fig. 15, the equilibrium gain is significantly under-predicted, and if the R.2 rates are adjusted to accurately predict the equilibrium gain, Fig. 16, the gain recovery slope is significantly over-predicted. This indicates that the R.1/R.2 mechanism cannot explain the deviation of gain recovery data from theory.

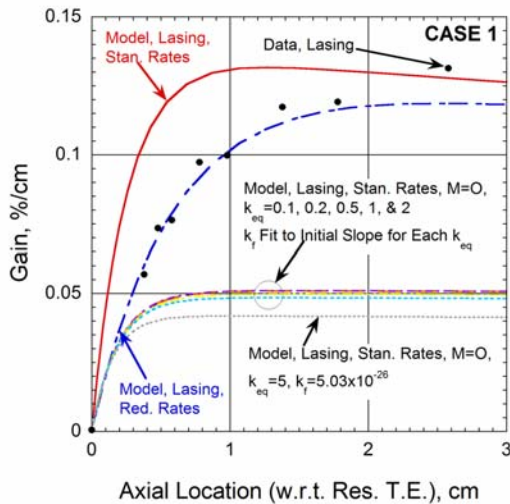


Fig 15. Gain recovery case 1 calculated gain as a function of 3-body $O_2(a^1\Delta) \leftrightarrow I^*$ energy transfer rates (not assuming $k_{eq1}=k_{eq2}$) and axial location compared to data as a function of axial location.

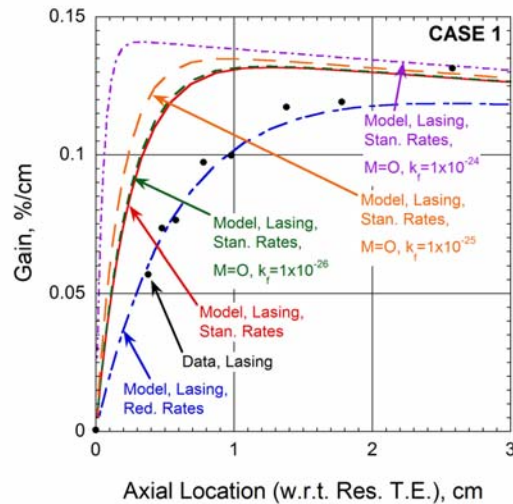
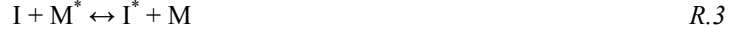


Fig 16. Gain recovery case 1 calculated gain as a function of 3-body $O_2(a^1\Delta) \leftrightarrow I^*$ energy transfer rates (assuming $k_{eq1}=k_{eq2}$) and axial location compared to data as a function of axial location.

An additional gain recovery inhibition mechanism is herein proposed in which I^* recovery is inhibited and/or further coupled to $O_2(a^1\Delta)$ via an excited state of an unidentified specie, M^* and M respectively, as a result of 2-body

processes R.3 and R.4. In this proposed mechanism, M^* is nearly resonant with I^* and $O_2(a^1\Delta)$. Due to the assumed near resonance between M^* and $I^*/O_2(a^1\Delta)$, this mechanism should result in minimal energy loss.



As data has indicated that any additional mechanism affecting gain recovery should produce an equilibrium gain value near that predicted by R.1 alone, the equation describing the $I^*/I \leftrightarrow O_2(a^1\Delta)/O_2$ equilibrium predicted by R.1,

$$k_{eq1} [I][O_2(a)] = [I^*][O_2] \Rightarrow \frac{[I^*]}{[I]} = k_{eq1} \frac{[O_2(a)]}{[O_2]} \quad E.3$$

was combined with the equation describing the $I^*/I \leftrightarrow M^*/M$ equilibrium predicted by R.3,

$$k_{eq3} [I][M^*] = [I^*][M] \Rightarrow \frac{[I^*]}{[I]} = k_{eq3} \frac{[M^*]}{[M]} \quad E.4$$

and the equation describing the $M^*/M \leftrightarrow O_2(a^1\Delta)/O_2$ equilibrium predicted by R.4,

$$k_{eq4} [M][O_2(a)] = [M^*][O_2] \Rightarrow \frac{[M^*]}{[M]} = k_{eq4} \frac{[O_2(a)]}{[O_2]} \quad E.5$$

to determine an equation that constrains k_{eq3} and k_{eq4} to satisfy the equilibrium gain requirement.

$$\frac{[I^*]}{[I]} = k_{eq3} \frac{[M^*]}{[M]} = k_{eq3} k_{eq4} \frac{[O_2(a)]}{[O_2]} \Rightarrow k_{eq1} = k_{eq3} k_{eq4} \quad E.6$$

To test the R.3/R.4 mechanism, a small 1 mmol/s flow rate of an unspecified specie M was added to the gain recovery case 1 mixture. Note that the standard case 1 mixture has a total flow rate near 500 mmol/s and therefore is not otherwise affected by the addition of a small flow rate. To satisfy the equilibrium gain requirement, E.6, $k_{eq3} = 1$ and $k_{eq4} = k_{eq1}$ were chosen. Note that this choice is not arbitrary as calculations (not shown for brevity) indicate that the choice of $k_{eq4} \approx 1$ and $k_{eq3} \approx k_{eq1}$ (or any choice in which $\log(k_{eq3}) \gg 1$ or $\log(k_{eq3}) \ll 1$) produces a system in which a significant change in I^*/I only gives rise to a small change in M^*/M , thereby limiting the influence of the additional mechanism. Three R.3/R.4 mechanism reaction subsets were modeled with the gain recovery case 1 scenario and are compared to data and calculations assuming only R.1 with standard and reduced rates, Fig. 17.

- i. R.4 is turned off
- ii. R.4 is slow with respect to R.3
- iii. R.4 is on the order of R.3

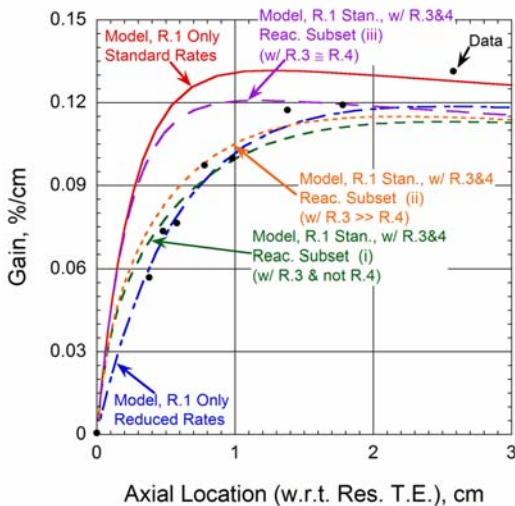


Fig 17. Gain recovery case 1 calculated gain as a function of 2-body $M^* \leftrightarrow I^*$ energy transfer rates and axial location compared to data as a function of axial location.

Calculations indicate that when R.4 is slow with respect to R.3 or off, reasonable agreement is obtained with gain recovery data, Fig. 17. In these two cases, as the post-lasing I^*/I equilibrium recovers, the M^*/M equilibrium recovers primarily via I^* and R.3, thereby inhibiting gain recovery. When R.4 is on the order of R.3, gain recovers at a rate similar to that predicted by R.1 alone as the M^*/M equilibrium is restored primarily via $O_2(a^1\Delta)$ and R.4 leaving I^* and gain recovery unaffected. Note that in all three R.3/R.4 mechanism reaction subsets, gain recovers to nearly the same equilibrium gain value slightly less than that predicted by R.1 alone, Fig. 17. This small difference is due to the small reduction in downstream $O_2(a^1\Delta)$ yield associated with a small energy flux held in the M^* state. Additional cases (not shown) have indicated that the R.3/R.4 mechanism can be used to match gain recovery for total M flow rates greater than approximately 1 mmol/s. $O_2/O_2(X, v=5)$ are among potential candidates for M/M^* due to the total O_2 flow rate and near resonance with $I^*/O_2(a^1\Delta)$. It is also possible that there are multiple species M_i that may play a role, e.g. $NO/NO(v=3)$; inclusion of multiple species M_i may also permit better agreement between the model and experimental data.

VI. Concluding Remarks

A baseline case simulation of the current best gain and power case is in good agreement with data other than laser power and post-lasing gain recovery rate. Measurements of gain recovery downstream of an operating laser cavity for five cases of interest were presented and modeled. Calculations indicated that multiplication of the forward and backward rates for the $O_2(a^1\Delta) \leftrightarrow I^*$ energy transfer reaction by a factor of approximately 0.3 permits the calculated post-lasing gain recovery rate to closely match data for all cases containing NO. A the $O_2(a^1\Delta) \leftrightarrow I^*$ energy transfer reaction rate multiplication factor of 0.56 was found to be optimum for the single case not containing NO. Calculations indicated that the actual unidentified mechanism inhibiting gain recovery must be near lossless and that diffraction and resonator region power flux or specie flux losses are not good candidates. Calculations further indicated that an additional proposed 3-body $O_2(a^1\Delta) \leftrightarrow I^*$ energy transfer reaction cannot explain the gain recovery data as this mechanism cannot simultaneously predict the reduced gain recovery rate and the downstream equilibrium gain. However, calculations using a proposed two reaction $O_2(a^1\Delta) \leftrightarrow I^*$ energy transfer mechanism dependent upon an unidentified excited state and specie M^* and M (or possibly multiple species M_i^* and M_i), may explain the gain recovery data. Further experiments and calculations are recommended.

Acknowledgments

This work was supported by DARPA prime contract HR0011-07-C-0054 on a subcontract from Physical Sciences Inc. (PSI). Additionally, J. Zimmerman and B. Woodard were supported in part by the Directed Energy Professional Society (DEPS) Scholarship Program. The authors gratefully acknowledge the contributions of: W.T. Rawlins, S.J. Davis, and S. Lee (PSI); M. Heaven (Emory Univ.); G.W. Sutton (SPARTA/Cobham Analytic Solutions); J. Mangano (DARPA); and R. Snead (U.S. Army SMDC).

The views, opinions, and/or findings contained in this article are those of the authors and should not be interpreted as representing the official views or policies, either expressed or implied, of the Defense Advanced Research Projects Agency or the Department of Defense. Distribution Statement A (approved for public release, distribution unlimited).

References

- Atkinson, R., Baulch, D.L., Cox, R.A., Hampson, R.F., Kerr, J.A., Rossi, M.J., Troe, J. (1997). "Evaluated Kinetic, Photochemical and Heterogeneous Data for Atmospheric Chemistry," *Journal of Physics and Chemistry Reference Data*, **26** no. 3 pp. 550-962.
- Azyazov, V. N. , Antonov, I. O., Ruffner, S. and Heaven, M. C. (2006). Proc. SPIE 6101, 6101C-53.
- Basco, N, Hunt, J.E. (1978). "The Recombination of Iodine Atoms in the Presence of Nitric Oxide" *Int. J. Chem. Kinet.* **10**.
- Benavides, G. F., Zimmerman, J. W., Woodard, B. S., Carroll, D. L., Palla, A. D., Day, M. T., Verdeyen, J. T., and Solomon, W. C., "Enhancement of electric oxygen-iodine laser performance using a rectangular discharge and longer gain length," *Appl. Phys. Lett.* **95**, 221112 (2009).
- Buben, S.N., Larin, I. K., Messineva, N. A. and Trofimova, E. M. (1990). *Kinet. Catal.* **31**, 973-977.
- Boeuf, J.P., Marode, E. (1982). "A Monte Carlo analysis of an electron swarm in a nonuniform field: the cathode region of a glow discharge in helium," *Journal of Physics D: Applied Physics*, **15** pp. 2169.
- Bruzzese J, Cole A, Nishihara M, and Adamovich I V (2009). "Gain Distribution and Output Power Measurements in a Scaled Electric Discharge Excited Oxygen-Iodine Laser," AIAA Paper 2009-4061.

- Burrow, P.D. (1973). "Dissociative attachment from the $O_2(a^1\Delta_g)$ state," *Journal of Chemical Physics*, **59** pp. 4922.
- Busch, G. (1981). *IEEE Journal of Quantum Electronics*, **17** no. 6 pp. 1128-1133.
- Campbell, I.M., Gray, C.N. (1973). "Rate Constants for $O(^3P)$ Recombination and Association with $N(^4S)$," *Chem. Phys. Lett.*, **18**.
- Carroll D L, Verdeyen J T, King D M, Zimmerman J W, Laystrom J K, Woodard B S, Richardson N, Kittell K, Kushner M J and Solomon W C (2004). *Appl. Phys. Lett.* **85** 1320.
- Carroll D L, Verdeyen J T, King D M, Zimmerman J, Laystrom J, Woodard B, Benavides G, Kittell K, Stafford D, Kushner M J and Solomon W C (2005). *Appl. Phys. Lett.* **86** 111104.
- Carroll D L, Benavides G F, Zimmerman J W, Woodard B S, Palla A D, Verdeyen J T, and Solomon W C (2009a). "Systematic development of the electric discharge oxygen-iodine laser," *SPIE Vol.* **7131**, 71310B.
- Carroll D L, and Verdeyen J T (2009b). *Applied Optics* **48** 6035.
- Deakin, J.J., Husain, D. (1972). *Journal of the Chemical Society*, **68** pp. 1603-1612.
- DeMore, W.B., Sander, S.P., Golden, D.M., Hampson, R.F., Kurylo, M.J., Howard, C.J., Ravishankara, A.R., Kolb, C.E., Molina, M.J. (1997). "Chemical kinetics and photochemical data for use in stratospheric modeling. Evaluation number 12" JPL Publication 97-4.
- Heaven, M.C. (2010). "Recent advances in the development of discharge-pumped oxygen-iodine lasers," *Laser Photonics Review*, to be published.
- Ebina, K., Yokozawa, T., Yamaguchi, S., Kanazawa, H., Hara, H., Mine, Y., Komatsu, K., Saito, H. (1994). "A New Kinetic Model for Assessing the Performance of Advanced CO_2 Gasdynamic Lasers" *Japanese Journal of Applied Physics*, **33** no. 3A pp. 1340-1345.
- Estupinan, E.G., Nicovich, J.M., Li, J., Cunnold, D.M., Wine, P.H. (2002). "Investigation of N_2O Production from 266 and 532 nm Laser Flash Photolysis of $O_3/N_2/O_2$ Mixtures," *J. Phys. Chem. A*, **106**.
- Findlay, F.D., Snelling, D.R. (1971). "Collisional deactivation of $O_2(a^1\Delta_g)$," *J. Chem. Phys.*, **55**.
- Fisher, E. (1997). "Calculations of the Effect of Nitrogen Vibrational Kinetics on Laminar Flame Temperature Profiles," *Combustion and Flame*, **108** no. 1-2 pp. 127-138.
- Forst, W., Evans, H.G.V., Winkler, C.A. (1957). "The kinetics of nitrogen atom reactions accompanied by catalyzed recombination of atoms," *J. Phys. Chem.*
- Gordiets, B.F., Ferreira, C.M., Guerra, V.L., Loureiro, J.M.A.H., Nahorny, J., Pagnon, D., Touzeau, M., Vialle, M. (1995). "Kinetic model of a low-pressure N_2-O_2 flowing glow discharge," *Plasma Science, IEEE Transactions*, **23** no. 4 pp. 750-768.
- Hall, R.I., Trajmar, S. (1975). "Scattering of 4.5 eV electrons by ground ($X^3\Sigma_g$) state and metastable ($a^1\Delta_g$) oxygen molecules," *Journal of Physics B*, **8** no. 12 pp. L293.
- Han, J., Komissarov, A.V., Tinney, S.P., Heaven, M.C. (2003). "Kinetic studies for advanced iodine laser concepts," *Proceedings of SPIE*, **4971** pp. 45-56.
- Han, J., Tinney, S.P., Heaven, M.C. (2004). "Kinetics of Relevance to Discharge Driven COIL Systems," *Proceedings of SPIE*, **5448** pp. 261-268.
- Heaven, M. (1995). "Studies of Energy Transfer Processes of Relevance to Chemically and Optically Pumped Lasers," Air Force Office of Scientific Research, Bolling Air Force Base, Final Report AFOSR-TR-95-0012.
- Herron, J.T. (1999). "Evaluated Chemical Kinetics Data for Reactions of $N(^2D)$, $N(^2P)$, and $N_2(A^3\Sigma)$ in the Gas Phase," *J. Phys. Chem. Ref. Data*, **28**.
- Herron, J.T., Green, D.S. (2001). "Chemical Kinetics Database and Predictive Schemes for Nonthermal Humid Air Plasma Chemistry. Part II. Neutral Species Reactions," *Plasma Chemistry and Plasma Processing*, **21** no. 3 pp. 459-481.
- Hicks A, Tirupathi S, Jiang N, Utkin Yu, Lempert W R, Rich J W and Adamovich I V (2007). *J. Phys. D: Appl. Phys.* **40** 1408.
- Hokazono, H., Obara, M., Midorikawa, K., Tashiro, H. (1991). "Theoretical Operational Life Study of the Closed-Cycle Transversely Excited Atmospheric CO_2 Laser," *Journal of Applied Physics*, **69** no. 10 pp. 6850-6868.
- Gonzalez, M., Sayos, R., Valero, R. (2002). "Ab Initio and Kinetics Study of the Ground Potential Energy Surface of the $O(^1D) + N_2O \rightarrow 2 NO, N_2 + O_2(a^1\Delta_g)$," *Chem. Phys. Lett.*, **355**.
- Ikezoe, Y., Matsuoka, S., Takeba, M., Viggiano, A. (1986). "Gas Phase Ion-Molecule Reaction Rate Constants Through 1986." *The Mass Spectroscopy Society of Japan*
- IUPAC Subcommittee for Gas Kinetic Data Evaluation (2010), <http://www.iupac-kinetic.ch.cam.ac.uk>.
- Ionin A A, Kochetov I V, Napartovich A P and Yuryshv N N, (2007). *J. Phys. D: Appl. Phys.* **40** R25.
- Kaufman, F. (1958). *Proceedings of the Royal Society A*, **247** pp. 123-139.
- Laher, R.R., Gilmore, F.R. (1990). "Updated Excitation and Ionization Cross Sections for Electron Impact on Atomic Oxygen," *Journal of Physical and Chemical Reference Data*, **19** pp. 277.

- Lesar, A., Senegacnik, M. (1993). "¹⁵N and ¹⁸O kinetic isotope effects in the thermal decomposition of N₂O catalyzed by bromine," *J. Chem. Phys.*, **99**.
- Matejcik, S., Kiendler, A., Cicman, P., Skalny, J., Stampfli, P., Illenberger, E., Chu, Y., Stamatovic, A., Mark, T.D. (1997). "Electron attachment to molecules and clusters of atmospheric relevance: oxygen and ozone," *Plasma Sources Science and Technology*, **6** no. 2 pp. 140.
- Mavroyannis, C., Winkler, C.A. (1961). "The reaction of active nitrogen with molecular oxygen," *Chem. React. Lower Upper Atmos. Proc. Int. Symp.*.
- Meagher, N.E., Anderson, W.R. (2000). "Kinetics of the O(³P) + N₂O Reaction. 2. Interpretation and Recommended Rate Coefficients," *J. Phys. Chem. A*, **104**.
- Mebel, A.M., Lin, M.C., Morokuma, K., Melius, C.F. (1996). "Theoretical study of reactions of N₂O with NO and OH radicals," *Int. J. Chem. Kinet.*, **28**.
- Mikheyev, P. A., Postell, D. J., and Heaven, M. C. (2009). "Temperature dependence of the O + I(²P_{1/2}) → O + I(²P_{3/2}) quenching rate constant," *Jour. Appl. Phys.* **105** 094911.
- Palla, A.D, Carroll, D. L., Verdeyen, J. T., and Solomon, W. C., (2006a) "Mixing Effects in Post-Discharge Modeling of Electric Discharge Oxygen-Iodine Laser Experiments," *Jour. Physics D*, **100**, 023117.
- Palla, A. D., Carroll, D. L., Verdeyen, J. T., and Solomon, W. C., (2006b) "Effects of Mixing on Post-Discharge Modeling of ElectricOIL Experiments," *Proc. SPIE*, **6101**, 610125.
- Palla, A. D., Zimmerman, J. W., Woodard, B. S., Carroll, D. L., Verdeyen, J. T., Lim, T. C., and Solomon, W. C., (2007a) "Oxygen Discharge and Post-Discharge Kinetics Experiments and Modeling for the Electric Oxygen-Iodine Laser System," *Jour. Phys. Chemistry A*, **111**, 6713-6721.
- Palla, A. D., Zimmerman, J. W., Woodard, B. S., Carroll, D. L., Verdeyen, J. T., Lim, T. C., Rawlins, W. T., Lee, S., Davis, S. J., and Solomon, W. C., (2007b) "ElectricOIL Discharge and Post-Discharge Kinetics Experiments and Modeling," *Proc. SPIE*, **6454**, 645401.
- Perram, G.P., Hager, G.D. (1988). "The Standard Chemical Oxygen-Iodine Laser Kinetics Package," Air Force Weapons Laboratory, Air Force System Command, Kirtland AFB, NM, Final Rep. AFWL-TR-88-50 pp. 127-138.
- Phelps, A.V. (1985). *JILA Information Center Report* **28**.
- Ralchenko, Yu., Kramida, A.E., Reader, J., and NIST ASD Team (2008). *NIST Atomic Spectra Database* (version 3.1.5), [Online]. Available: <http://physics.nist.gov/asd3> [2010, May 14]. National Institute of Standards and Technology, Gaithersburg, MD.
- Rapp, D., Englander-Golden, P. (1965). "Total Cross Sections for Ionization and Attachment in Gases by Electron Impact. I. Positive Ionization," *Journal of Chemical Physics*, **43** pp. 1464.
- Rawlins W T, Lee S, Kessler W J and Davis S J (2005). *Appl. Phys. Lett.* **86** 051105.
- Shi, J., Barker, J.R. (1990). "Kinetic studies of the deactivation of O₂(a¹Δ_g) and O(¹D)," *International Journal of Chemical Kinetics*, **22** no. 12 pp. 1283-1301.
- Solomon, W. C. (2010), *Private Communication*.
- Stafford, D. S., and Kushner, M. J. (2004). "O₂(¹A) production in flowing He/O₂ mixtures in flowing low pressure plasmas," *J. Appl. Phys.*, **96**, no. 5 pp. 2451.
- Stafford, D. S., and Kushner, M. J., "O₂(¹Δ) production in flowing He/O₂ plasmas. I. Axial transport and pulsed power formats," *J. Appl. Phys.*, **98**, 073303 (2006).
- Van Den Bergh, H., Troe, J. (1975). "NO-catalyzed Recombination of Iodine Atoms: Elementary steps of the Complex Mechanism." *Chem. Phys. Lett* **31**, 351-354.
- Van Den Bergh, H., and Troe, J. (1976). *J. Chem. Phys.* **64**, 736.
- Van Marter, T., and Heaven, M. C. (1998), "I(²P_{1/2})+O₂: Studies of low-temperature electronic energy transfer and nuclear spin-state changing collisions," *J. Chem. Phys.*, Vol. 109, No. 21, p. 9266.
- Van Marter, T., Heaven, M. C., and Plummer, D. (1996), *Chem. Phys. Lett.*, **260**, 201.
- Vasiljeva, A.N., Klopovskiy, K.S., Kovalev, A.S., Lopaev, D.V., Mankelevich, Y.A., Popov, N.A., Rakhimov, A.T., Rakhimova, T.V. (2004). "On the possibility of O₂(a¹Δ_g) production by a non-self-sustained discharge for oxygen-iodine laser pumping," *Journal of Physics D: Applied Physics*, **37** no. 17 pp. 2455.
- Verdeyen J. T., Carroll, D. L., King, D. M., Laystrom, J., Benavides, G., Zimmerman, J., Woodard, B., and Solomon, W. C., "Continuous-wave laser oscillation in subsonic flow on the 1315 nm atomic iodine transition pumped by electric discharge produced O₂(¹Δ)," *Appl. Phys. Lett.* **89** 101115 (2006).
- Vriens, L. (1964). "Calculation of absolute ionisation cross sections of He, He*, He⁺, Ne, Ne*, Ne⁺, Ar, Ar*, Hg and Hg*," *Physics Letters*, **8** no. 4 pp. 260-261.
- Wennberg, P.O., Anderson, J.G., Weisenstein, D.K. (1994). "Kinetics of reactions of ground state nitrogen atoms with NO and NO₂," *J. Geophys. Res.*, **99**.

- Woodard B S, Zimmerman J W, Benavides G F, Carroll D L, Verdeyen J T, Palla A D, Field T H, Solomon W C, Davis S J, Rawlins W T, and Lee S (2008). *Appl. Phys. Lett.* **93** 021104.
- Woodard, B. S., Benavides, G. F., Zimmerman, J. W., Carroll, D. L., Palla, A. D., Day, M. T., Verdeyen, J. T., and Solomon, W. C., "Enhancement of electric oxygen-iodine laser performance using larger mode volume resonators," *Opt. Lett.* to be published (2010).
- Zimmerman J W, Woodard B S, Benavides G F, Carroll D L, Verdeyen J T, Palla A D and Solomon W C (2008). *Appl. Phys. Lett.* **92** 241115.
- Zimmerman J W, Benavides G F, Palla A D, Woodard B S, Carroll D L, Verdeyen J T, and Solomon W C (2009). "Gain recovery in an electric oxygen-iodine laser," *Appl. Phys. Lett.* **94** 021109.
- Zuev, A.P., Starikovskii, A.Y. (1991). "Reactions involving nitrogen oxides at high temperatures. The reaction of N₂O with O," *Khim. Fiz.*, **10**.

Appendix 1 Reaction set used in BLAZE-IV ElectricOIL calculations. Note that reaction rate units are $\text{cm}^3/\text{molecule}\cdot\text{s}$ and $\text{cm}^6/\text{molecule}^2\cdot\text{s}$ for two and three-body reactions respectively. († Denotes a reaction and rate derived from a similar reaction. ‡ Denotes a reaction and rate derived to best fit data. \rightarrow and \leftrightarrow Denote one-way and reversible reactions respectively).

<i>n</i>	<i>Reaction</i>	<i>Rate</i>	<i>Reference</i>
1	$\text{Ar} + \text{I}^2\text{P}_{1/2} \rightarrow \text{Ar} + \text{I}^2\text{P}_{3/2}$	5×10^{-18}	†
2	$\text{Ar} + \text{I}_2(v=20) \rightarrow \text{Ar} + \text{I}_2$	3.99×10^{-12}	Perram,1988
3	$\text{Ar} + \text{O}_2(\text{a}^1\Delta) \rightarrow \text{Ar} + \text{O}_2(^3\text{X})$	1×10^{-19}	Stafford,2004
4	$\text{Ar} + \text{O}_2(\text{b}^1\Sigma) \rightarrow \text{Ar} + \text{O}_2(\text{a}^1\Delta)$	1×10^{-17}	Ionin,2003
5	$\text{He} + 2 \text{I}^2\text{P}_{3/2} \rightarrow \text{He} + \text{I}_2$	3.81×10^{-33}	Busch,1978
6	$\text{He} + \text{I}^2\text{P}_{1/2} \rightarrow \text{He} + \text{I}^2\text{P}_{3/2}$	5×10^{-18}	Perram,1988
7	$\text{He} + \text{I}_2(v=20) \rightarrow \text{He} + \text{I}_2$	9.8×10^{-12}	Heaven,1995
8	$\text{He} + \text{O}_2(^3\text{X},v=1) \leftrightarrow \text{He} + \text{O}_2(^3\text{X})$	1.3×10^{-13}	Atkinson,1997
10	$\text{He} + \text{O}_2(^3\text{X},v=2) \leftrightarrow \text{He} + \text{O}_2(^3\text{X},v=1)$	1.3×10^{-13}	†
12	$\text{He} + \text{O}_2(^3\text{X},v=3) \leftrightarrow \text{He} + \text{O}_2(^3\text{X},v=2)$	1.3×10^{-13}	†
14	$\text{He} + \text{O}_2(^3\text{X},v=4) \leftrightarrow \text{He} + \text{O}_2(^3\text{X},v=3)$	1.3×10^{-13}	†
16	$\text{He} + \text{O}_2(^3\text{X},v=5) \leftrightarrow \text{He} + \text{O}_2(^3\text{X},v=4)$	1.3×10^{-13}	†
18	$\text{I}^2\text{P}_{3/2} + \text{I}^2\text{P}_{1/2} \rightarrow 2 \text{I}^2\text{P}_{3/2}$	1.69×10^{-13}	Perram,1988
19	$\text{I}^2\text{P}_{3/2} + \text{I}^2\text{P}_{1/2} + \text{I}_2 \rightarrow \text{I}_2 + 2 \text{I}^2\text{P}_{3/2}$	3.61×10^{-30}	Perram,1988
20	$\text{I}^2\text{P}_{3/2} + \text{I}^2\text{P}_{1/2} + \text{I}_2 \rightarrow \text{I}_2 + \text{I}_2(^3\Pi_{0+U})$	3.61×10^{-30}	Perram,1988
21	$\text{I}^2\text{P}_{3/2} + \text{O}_2(\text{a}^1\Delta) \rightarrow \text{I}^2\text{P}_{3/2} + \text{O}_2(^3\text{X})$	1×10^{-15}	Perram,1988
22	$\text{I}^2\text{P}_{1/2} + \text{N}_2 \rightarrow \text{I}^2\text{P}_{3/2} + \text{N}_2$	6.5×10^{-17}	Deakin,1972
23	$\text{I}^2\text{P}_{1/2} + \text{O}_2(^3\text{X}) \rightarrow \text{I}^2\text{P}_{3/2} + \text{O}_2(^3\text{X})$	3.49×10^{-16}	Perram,1988
24	$\text{I}^2\text{P}_{1/2} + \text{O}_2(\text{a}^1\Delta) \rightarrow \text{I}^2\text{P}_{3/2} + \text{O}_2(\text{a}^1\Delta)$	1.09×10^{-13}	Perram,1988
25	$\text{I}^2\text{P}_{1/2} + \text{Xe} \rightarrow \text{I}^2\text{P}_{3/2} + \text{Xe}$	5×10^{-18}	†
26	$\text{I}_2 + 2 \text{I}^2\text{P}_{3/2} \rightarrow 2 \text{I}_2$	3.61×10^{-30}	Perram,1988
27	$\text{I}_2 + \text{O}_2(\text{a}^1\Delta) \rightarrow \text{I}_2 + \text{O}_2(^3\text{X})$	5×10^{-16}	Han,2003
28	$\text{I}_2 + \text{O}_2(\text{b}^1\Sigma) \rightarrow \text{I}_2 + \text{O}_2(^3\text{X})$	6×10^{-12}	Heaven,1995
29	$\text{I}_2 + \text{O}_2(\text{b}^1\Sigma) \rightarrow \text{I}_2 + \text{O}_2(\text{a}^1\Delta)$	2.31×10^{-11}	Han,2003
30	$\text{I}_2(^3\Pi_{0+U}) \rightarrow 2 \text{I}^2\text{P}_{3/2}$	1×10^6	Perram,1988
31	$\text{I}_2(v=20) + \text{Xe} \rightarrow \text{I}_2 + \text{Xe}$	3.99×10^{-12}	Busch, 1981
32	$\text{N}_2 + 2 \text{I}^2\text{P}_{3/2} \rightarrow \text{I}_2 + \text{N}_2$	4.18×10^{-32}	Busch, 1981
33	$\text{N}_2 + \text{O}_2(\text{a}^1\Delta) \rightarrow \text{N}_2 + \text{O}_2(^3\text{X})$	1.4×10^{-19}	Atkinson,1997
34	$\text{N}_2 + \text{O}_2(\text{b}^1\Sigma) \rightarrow \text{N}_2 + \text{O}_2(^3\text{X})$	1.99×10^{-16}	Atkinson,1997
35	$\text{N}_2 + \text{O}_2(\text{b}^1\Sigma) \rightarrow \text{N}_2 + \text{O}_2(\text{a}^1\Delta)$	1.79×10^{-15}	Atkinson,1977
36	$\text{O}_2(^3\text{X}) + 2 \text{I}^2\text{P}_{3/2} \rightarrow \text{I}_2 + \text{O}_2(^3\text{X})$	3.33×10^{-32}	Han,2003
37	$\text{O}_2(^3\text{X}) + 2 \text{I}^2\text{P}_{3/2} \rightarrow \text{I}_2 + \text{O}_2(\text{a}^1\Delta)$	3.7×10^{-33}	Han,2003
38	$\text{O}_2(^3\text{X}) + \text{O}_2(^3\text{X},v=1) \leftrightarrow 2 \text{O}_2(^3\text{X})$	3.99×10^{-14}	Atkinson,1997
40	$\text{O}_2(^3\text{X}) + \text{O}_2(^3\text{X},v=2) \leftrightarrow \text{O}_2(^3\text{X}) + \text{O}_2(^3\text{X},v=1)$	3.99×10^{-14}	†
42	$\text{O}_2(^3\text{X}) + \text{O}_2(^3\text{X},v=3) \leftrightarrow \text{O}_2(^3\text{X}) + \text{O}_2(^3\text{X},v=2)$	3.99×10^{-14}	†
44	$\text{O}_2(^3\text{X}) + \text{O}_2(^3\text{X},v=4) \leftrightarrow \text{O}_2(^3\text{X}) + \text{O}_2(^3\text{X},v=3)$	3.99×10^{-14}	†
46	$\text{O}_2(^3\text{X}) + \text{O}_2(^3\text{X},v=5) \leftrightarrow \text{O}_2(^3\text{X}) + \text{O}_2(^3\text{X},v=4)$	3.99×10^{-14}	†
48	$\text{O}_2(\text{a}^1\Delta) + \text{Xe} \rightarrow \text{O}_2(^3\text{X}) + \text{Xe}$	1×10^{-19}	†
49	$\text{O}_2(\text{b}^1\Sigma) + \text{Xe} \rightarrow \text{O}_2(\text{a}^1\Delta) + \text{Xe}$	1×10^{-17}	Ionin,2003
50	$\text{H}_2\text{O} + \text{O}_2(\text{a}^1\Delta) \rightarrow \text{H}_2\text{O} + \text{O}_2(^3\text{X})$	4×10^{-18}	Perram,1988
51	$\text{He} + \text{O}_2(\text{a}^1\Delta) \rightarrow \text{He} + \text{O}_2(^3\text{X})$	8×10^{-21}	Perram,1988
52	$\text{He} + \text{O}_2(\text{b}^1\Sigma) \rightarrow \text{He} + \text{O}_2(\text{a}^1\Delta)$	1×10^{-17}	Perram,1988
53	$\text{O}_2(^3\text{X}) + \text{O}_2(\text{a}^1\Delta) \rightarrow 2 \text{O}_2(^3\text{X})$	8.21×10^{-19}	Han,2003
54	$\text{O}_2(^3\text{X}) + \text{O}_2(\text{b}^1\Sigma) \rightarrow \text{O}_2(^3\text{X}) + \text{O}_2(\text{a}^1\Delta)$	3.7×10^{-17}	Han,2003

55	$O_2(^3X) + O_2(b^1\Sigma) \rightarrow 2 O_2(^3X)$	$2.3 \times 10^{-19} T^{0.5}$	Atkinson, 1997
56	$2 O_2(a^1\Delta) \rightarrow O_2(^3X) + O_2(b^1\Sigma)$	$9.8 \times 10^{-28} T^{3.800} \exp(700/T)$	Perram, 1988
57	$2 O_2(a^1\Delta) \rightarrow 2 O_2(^3X)$	1.69×10^{-17}	Perram, 1988
58	$2 O_2(b^1\Sigma) \rightarrow O_2(^3X) + O_2(a^1\Delta)$	$2.07 \times 10^{-18} T^{0.5}$	‡
59	$H_2O + O_2(b^1\Sigma) \rightarrow H_2O + O_2(a^1\Delta)$	6.71×10^{-12}	Perram, 1988
60	$H_2O + I(^2P_{1/2}) \rightarrow H_2O + I(^2P_{3/2})$	2.11×10^{-12}	Perram, 1988
61	$H_2O + I_2(v=20) \rightarrow H_2O + I_2$	1.69×10^{-11}	Heaven, 1995
62	$I(^2P_{3/2}) + O_2(a^1\Delta) \rightarrow I(^2P_{1/2}) + O_2(^3X)$	$6.28 \times 10^{-12} T^{0.5}$	Van Marter, 1998
63	$I(^2P_{1/2}) + I_2 \rightarrow I(^2P_{3/2}) + I_2(v=20)$	$1.4 \times 10^{-13} \exp(1600/T)$	Perram, 1988
64	$I(^2P_{1/2}) + O_2(^3X) \rightarrow I(^2P_{3/2}) + O_2(a^1\Delta)$	$8.39 \times 10^{-12} T^{0.5} \exp(-403/T)$	Van Marter, 1998
65	$I(^2P_{1/2}) + O_2(a^1\Delta) \rightarrow I(^2P_{3/2}) + O_2(b^1\Sigma)$	$4 \times 10^{-24} T^{3.800} \exp(700/T)$	Perram, 1988
66	$I_2 + O_2(a^1\Delta) \rightarrow I_2(v=20) + O_2(^3X)$	7.01×10^{-15}	Perram, 1988
67	$I_2 + O_2(b^1\Sigma) \rightarrow O_2(^3X) + 2 I(^2P_{3/2})$	2.81×10^{-11}	Heaven, 2005
68	$I_2(v=20) + N_2 \rightarrow I_2 + N_2$	8.16×10^{-12}	Heaven, 1996
69	$I_2(v=20) + O_2(^3X) \rightarrow I_2 + O_2(^3X)$	4.9×10^{-12}	Heaven, 1995
70	$I_2(v=20) + O_2(a^1\Delta) \rightarrow O_2(^3X) + 2 I(^2P_{3/2})$	3.01×10^{-10}	Perram, 1988
71	$H_2O + O_2(a^1\Delta, v=1) \leftrightarrow H_2O + O_2(a^1\Delta)$	1.7×10^{-12}	Waichman, 2007
73	$H_2O + O_2(a^1\Delta, v=2) \leftrightarrow H_2O + O_2(a^1\Delta, v=1)$	1.7×10^{-12}	†
75	$H_2O + O_2(a^1\Delta, v=3) \leftrightarrow H_2O + O_2(a^1\Delta, v=2)$	1.7×10^{-12}	†
77	$H_2O + O_2(a^1\Delta, v=4) \leftrightarrow H_2O + O_2(a^1\Delta, v=3)$	1.7×10^{-12}	†
79	$H_2O + O_2(a^1\Delta, v=5) \leftrightarrow H_2O + O_2(a^1\Delta, v=4)$	1.7×10^{-12}	†
81	$H_2O + O_2(b^1\Sigma, v=1) \leftrightarrow H_2O + O_2(b^1\Sigma)$	1.7×10^{-12}	†
83	$H_2O + O_2(b^1\Sigma, v=2) \leftrightarrow H_2O + O_2(b^1\Sigma, v=1)$	1.7×10^{-12}	†
85	$H_2O + O_2(b^1\Sigma, v=3) \leftrightarrow H_2O + O_2(b^1\Sigma, v=2)$	1.7×10^{-12}	†
87	$H_2O + O_2(b^1\Sigma, v=4) \leftrightarrow H_2O + O_2(b^1\Sigma, v=3)$	1.7×10^{-12}	†
89	$H_2O + O_2(b^1\Sigma, v=5) \leftrightarrow H_2O + O_2(b^1\Sigma, v=4)$	1.7×10^{-12}	†
91	$H_2O + O_2(^3X, v=1) \leftrightarrow H_2O + O_2(^3X)$	1.7×10^{-12}	Waichman, 2007
93	$H_2O + O_2(^3X, v=2) \leftrightarrow H_2O + O_2(^3X, v=1)$	1.7×10^{-12}	†
95	$H_2O + O_2(^3X, v=3) \leftrightarrow H_2O + O_2(^3X, v=2)$	1.7×10^{-12}	†
97	$H_2O + O_2(^3X, v=4) \leftrightarrow H_2O + O_2(^3X, v=3)$	1.7×10^{-12}	†
99	$H_2O + O_2(^3X, v=5) \leftrightarrow H_2O + O_2(^3X, v=4)$	1.7×10^{-12}	†
101	$O_2(a^1\Delta) + O_2(^3X, v=1) \leftrightarrow O_2(^3X) + O_2(a^1\Delta, v=1)$	7.89×10^{-11}	Waichman, 2007
103	$O_2(a^1\Delta) + O_2(^3X, v=2) \leftrightarrow O_2(^3X) + O_2(a^1\Delta, v=2)$	7.3×10^{-11}	Waichman, 2007
105	$O_2(a^1\Delta) + O_2(^3X, v=3) \leftrightarrow O_2(^3X) + O_2(a^1\Delta, v=3)$	6.99×10^{-11}	Waichman, 2007
107	$O_2(a^1\Delta, v=1) + O_2(a^1\Delta, v=2) \leftrightarrow O_2(a^1\Delta) + O_2(a^1\Delta, v=3)$	2.6×10^{-13}	†
109	$O_2(a^1\Delta, v=1) + O_2(a^1\Delta, v=3) \leftrightarrow O_2(a^1\Delta) + O_2(a^1\Delta, v=4)$	2.6×10^{-13}	†
111	$O_2(a^1\Delta, v=1) + O_2(a^1\Delta, v=4) \leftrightarrow O_2(a^1\Delta) + O_2(a^1\Delta, v=5)$	2.6×10^{-13}	†
113	$2 O_2(a^1\Delta, v=1) \leftrightarrow O_2(a^1\Delta) + O_2(a^1\Delta, v=2)$	1.99×10^{-13}	†
115	$O_2(a^1\Delta, v=2) + O_2(a^1\Delta, v=3) \leftrightarrow O_2(a^1\Delta, v=1) + O_2(a^1\Delta, v=4)$	2.6×10^{-13}	†
117	$O_2(a^1\Delta, v=2) + O_2(a^1\Delta, v=4) \leftrightarrow O_2(a^1\Delta, v=1) + O_2(a^1\Delta, v=5)$	2.6×10^{-13}	†
119	$2 O_2(a^1\Delta, v=2) \leftrightarrow O_2(a^1\Delta, v=1) + O_2(a^1\Delta, v=3)$	2.6×10^{-13}	†
121	$O_2(a^1\Delta, v=3) + O_2(a^1\Delta, v=4) \leftrightarrow O_2(a^1\Delta, v=2) + O_2(a^1\Delta, v=5)$	2.6×10^{-13}	†
123	$2 O_2(a^1\Delta, v=3) \leftrightarrow O_2(a^1\Delta, v=2) + O_2(a^1\Delta, v=4)$	2.6×10^{-13}	†
125	$2 O_2(a^1\Delta, v=4) \leftrightarrow O_2(a^1\Delta, v=3) + O_2(a^1\Delta, v=5)$	2.6×10^{-13}	†
127	$O_2(b^1\Sigma) + O_2(^3X, v=1) \leftrightarrow O_2(^3X) + O_2(b^1\Sigma, v=1)$	2.5×10^{-11}	Waichman, 2007
129	$O_2(b^1\Sigma) + O_2(^3X, v=2) \leftrightarrow O_2(^3X) + O_2(b^1\Sigma, v=2)$	4.73×10^{-12}	Waichman, 2007
131	$O_2(b^1\Sigma, v=1) + O_2(b^1\Sigma, v=2) \leftrightarrow O_2(b^1\Sigma) + O_2(b^1\Sigma, v=3)$	2.6×10^{-13}	†
133	$O_2(b^1\Sigma, v=1) + O_2(b^1\Sigma, v=3) \leftrightarrow O_2(b^1\Sigma) + O_2(b^1\Sigma, v=4)$	2.6×10^{-13}	†
135	$O_2(b^1\Sigma, v=1) + O_2(b^1\Sigma, v=4) \leftrightarrow O_2(b^1\Sigma) + O_2(b^1\Sigma, v=5)$	2.6×10^{-13}	†
137	$2 O_2(b^1\Sigma, v=1) \leftrightarrow O_2(b^1\Sigma) + O_2(b^1\Sigma, v=2)$	1.99×10^{-13}	†

139	$O_2(b^1\Sigma, v=2) + O_2(b^1\Sigma, v=3) \leftrightarrow O_2(b^1\Sigma, v=1) + O_2(b^1\Sigma, v=4)$	2.6×10^{-13}	†
141	$O_2(b^1\Sigma, v=2) + O_2(b^1\Sigma, v=4) \leftrightarrow O_2(b^1\Sigma, v=1) + O_2(b^1\Sigma, v=5)$	2.6×10^{-13}	†
143	$2 O_2(b^1\Sigma, v=2) \leftrightarrow O_2(b^1\Sigma, v=1) + O_2(b^1\Sigma, v=3)$	2.6×10^{-13}	†
145	$O_2(b^1\Sigma, v=3) + O_2(b^1\Sigma, v=4) \leftrightarrow O_2(b^1\Sigma, v=2) + O_2(b^1\Sigma, v=5)$	2.6×10^{-13}	†
147	$2 O_2(b^1\Sigma, v=3) \leftrightarrow O_2(b^1\Sigma, v=2) + O_2(b^1\Sigma, v=4)$	2.6×10^{-13}	†
149	$2 O_2(b^1\Sigma, v=4) \leftrightarrow O_2(b^1\Sigma, v=3) + O_2(b^1\Sigma, v=5)$	2.6×10^{-13}	†
151	$O_2(^3X, v=1) + O_2(^3X, v=2) \leftrightarrow O_2(^3X) + O_2(^3X, v=3)$	2.6×10^{-13}	Waichman,2007
153	$O_2(^3X, v=1) + O_2(^3X, v=3) \leftrightarrow O_2(^3X) + O_2(^3X, v=4)$	2.6×10^{-13}	†
155	$O_2(^3X, v=1) + O_2(^3X, v=4) \leftrightarrow O_2(^3X) + O_2(^3X, v=5)$	2.6×10^{-13}	†
157	$2 O_2(^3X, v=1) \leftrightarrow O_2(^3X) + O_2(^3X, v=2)$	1.99×10^{-13}	Waichman,2007
159	$O_2(^3X, v=2) + O_2(^3X, v=3) \leftrightarrow O_2(^3X, v=1) + O_2(^3X, v=4)$	2.6×10^{-13}	†
161	$O_2(^3X, v=2) + O_2(^3X, v=4) \leftrightarrow O_2(^3X, v=1) + O_2(^3X, v=5)$	2.6×10^{-13}	†
163	$2 O_2(^3X, v=2) \leftrightarrow O_2(^3X, v=1) + O_2(^3X, v=3)$	2.6×10^{-13}	†
165	$O_2(^3X, v=3) + O_2(^3X, v=4) \leftrightarrow O_2(^3X, v=2) + O_2(^3X, v=5)$	2.6×10^{-13}	†
167	$2 O_2(^3X, v=3) \leftrightarrow O_2(^3X, v=2) + O_2(^3X, v=4)$	2.6×10^{-13}	†
169	$2 O_2(^3X, v=4) \leftrightarrow O_2(^3X, v=3) + O_2(^3X, v=5)$	2.6×10^{-13}	†
171	$Ar + O(^3P) + O_2(^3X) \rightarrow Ar + O_3$	$5.19 \times 10^{-27} T^{-2.800}$	†
172	$Ar + 2 O(^3P) \rightarrow Ar + O_2(^3X)$	$4.5 \times 10^{-34} \exp(630/T)$	†
173	$Ar(2p^1) \rightarrow Ar$	4.45×10^7	Ralchencko,2008
174	$Ar(2p^5) \rightarrow Ar$	4.02×10^7	Ralchencko,2008
175	$Ar(2p^7) \rightarrow Ar$	6.68×10^7	Ralchencko,2008
176	$Ar(2p^9) \rightarrow Ar$	6.68×10^7	Ralchencko,2008
177	$CO_2 + O_2(b^1\Sigma) \rightarrow CO_2 + O_2(a^1\Delta)$	4.1×10^{-13}	Atkinson,1997
178	$He + He^+ \rightarrow He + He^+$	$5.77 \times 10^{-11} T^{0.5}$	‡
179	$He + He^+ + O^- \rightarrow O(^3P) + 2 He$	$3.11 \times 10^{-19} T^{-2.5}$	‡
180	$He + NO + O(^3P) \rightarrow He + NO_2$	$2.07 \times 10^{-28} T^{-1.41}$	‡
181	$He + O(^3P) + O^+ \rightarrow He + O_2^+$	$5.77 \times 10^{-31} T^{0.5}$	‡
182	$He + O(^3P) + O_2(^3X) \rightarrow He + O_3$	$5.19 \times 10^{-27} T^{-2.8}$	Atkinson,1997
183	$He + 2 O(^3P) \rightarrow He + O_2(^3X)$	$4.5 \times 10^{-34} \exp(630/T)$	Herron, 2001
184	$He + 2 O(^3P) \rightarrow He + O_2(a^1\Delta)$	9.87×10^{-35}	Gordiets,1995
185	$He + O^+ + O^- \rightarrow He + 2 O(^3P)$	$3.11 \times 10^{-19} T^{-2.5}$	‡
186	$He + O^- + O_2^+ \rightarrow He + O(^3P) + O_2(^3X)$	$3.11 \times 10^{-19} T^{-2.5}$	‡
187	$He + O(^1D) \rightarrow He + O(^3P)$	9.99×10^{-14}	Shi,1990
188	$He + O(^1D) + O_2(^3X) \rightarrow He + O_3$	$5.19 \times 10^{-27} T^{-2.8}$	‡
189	$He + O_3 \rightarrow He + O(^3P) + O_2(^3X)$	$1.56 \times 10^{-9} \exp(-11490/T)$	‡
190	$He^* + O(^3P) \rightarrow He + O^+ + e^-$	$1.46 \times 10^{-11} T^{0.5}$	Stafford, 2004
191	$He^* + O(^1D) \rightarrow He + O^+ + e^-$	$1.46 \times 10^{-11} T^{0.5}$	Stafford, 2004
192	$He^* + O(^1S) \rightarrow He + O^+ + e^-$	$1.46 \times 10^{-11} T^{0.5}$	Stafford, 2004
193	$He^* + O_2(^3X) \rightarrow He + O_2^+ + e^-$	$1.46 \times 10^{-11} T^{0.5}$	Stafford, 2004
194	$He^* + O_2(b^1\Sigma) \rightarrow He + O_2^+ + e^-$	$1.46 \times 10^{-11} T^{0.5}$	Stafford, 2004
195	$He^* + O_3 \rightarrow He + O(^3P) + O_2^+ + e^-$	$1.46 \times 10^{-11} T^{0.5}$	Stafford, 2004
196	$2 He^* \rightarrow He + He^+ + e^-$	$8.66 \times 10^{-11} T^{0.5}$	Stafford, 2004
197	$He^+ + O(^3P) \rightarrow He + O^+$	$2.88 \times 10^{-12} T^{0.5}$	Stafford, 2004
198	$He^+ + O^- \rightarrow He + O(^3P)$	$6 \times 10^{-5} T^{-1}$	Gordiets,1995
199	$He^+ + O^- + O_2(^3X) \rightarrow He + O(^3P) + O_2(^3X)$	$3.11 \times 10^{-19} T^{-2.5}$	Gordiets,1995
200	$He^+ + O(^1D) \rightarrow He + O^+$	$2.88 \times 10^{-12} T^{0.5}$	Stafford, 2004
201	$He^+ + O(^1S) \rightarrow He + O^+$	$2.88 \times 10^{-12} T^{0.5}$	Stafford, 2004
202	$He^+ + O_2(^3X) \rightarrow He + O(^3P) + O^+$	$6.17 \times 10^{-11} T^{0.5}$	Stafford, 2004
203	$He^+ + O_2(^3X) \rightarrow He + O_2^+$	$1.9 \times 10^{-12} T^{0.5}$	Stafford, 2004
204	$He^+ + O_2^- \rightarrow He + O_2(^3X)$	$6 \times 10^{-5} T^{-1}$	Gordiets,1995

205	$\text{He}^+ + \text{O}_2(\text{a}^1\Delta) \rightarrow \text{He} + \text{O}(\text{^3P}) + \text{O}^+$	$6.17 \times 10^{-11} \text{ T}^{0.5}$	Stafford, 2004
206	$\text{He}^+ + \text{O}_2(\text{a}^1\Delta) \rightarrow \text{He} + \text{O}_2^+$	$1.9 \times 10^{-12} \text{ T}^{0.5}$	Stafford, 2004
207	$\text{He}^+ + \text{O}_3 \rightarrow \text{He} + \text{O}^+ + \text{O}_2(\text{^3X})$	$6.17 \times 10^{-11} \text{ T}^{0.5}$	Gordiets,1995
208	$\text{He}^+ + \text{O}_3^- \rightarrow \text{He} + \text{O}_3$	$6 \times 10^{-5} \text{ T}^{-1}$	Gordiets,1995
209	$\text{I}(\text{^2P}_{3/2}) + \text{INO} \rightarrow \text{I}_2 + \text{NO}$	1.66×10^{-10}	Basco, 1976
210	$\text{I}(\text{^2P}_{3/2}) + \text{INO}_2 \rightarrow \text{I}_2 + \text{NO}_2$	8.32×10^{-11}	Van Den Bergh, 1976
211	$\text{I}(\text{^2P}_{3/2}) + \text{N}_2 + \text{NO} \rightarrow \text{INO} + \text{N}_2$	$5.36 \times 10^{-30} \text{ T}^{-1}$	Atkinson, 1997
212	$\text{I}(\text{^2P}_{3/2}) + \text{NO} + \text{M} \rightarrow \text{INO} + \text{M}$	5.5×10^{-33}	Van Den Bergh, 1975
213	$\text{I}(\text{^2P}_{3/2}) + \text{NO}_2 + \text{M} \rightarrow \text{INO}_2 + \text{M}$	1.68×10^{-31}	Buben, 1990
214	$\text{I}(\text{^2P}_{3/2}) + \text{O}_3 \rightarrow \text{IO} + \text{O}_2(\text{^3X})$	$1.99 \times 10^{-11} \exp(-890/\text{T})$	Atkinson,1997
215	$\text{I}(\text{^2P}_{1/2}) + \text{NO} \rightarrow \text{I}(\text{^2P}_{3/2}) + \text{NO}$	1.2×10^{-13}	Heaven, 2004
216	$\text{I}(\text{^2P}_{1/2}) + \text{NO}_2 \rightarrow \text{I}(\text{^2P}_{3/2}) + \text{NO}_2$	8.5×10^{-14}	Han, 2004
217	$\text{I}(\text{^2P}_{1/2}) + \text{O}(\text{^3P}) \rightarrow \text{I}(\text{^2P}_{3/2}) + \text{O}(\text{^3P})$	$6.5 \times 10^{-12} (\text{T}/300)^{1.76}$	Mikheyev, 2009
218	$\text{I}_2 + \text{O}(\text{^3P}) \rightarrow \text{I}(\text{^2P}_{3/2}) + \text{IO}$	1.99×10^{-11}	IUPAC, 2010
219	$2 \text{INO} \rightarrow \text{I}_2 + 2 \text{NO}$	8.32×10^{-11}	Atkinson,1997
220	$2 \text{INO}_2 \rightarrow \text{I}_2 + 2 \text{NO}_2$	1.66×10^{-13}	IUPAC, 2010
221	$\text{IO} + \text{O}(\text{^3P}) \rightarrow \text{I}(\text{^2P}_{3/2}) + \text{O}_2(\text{^3X})$	1.35×10^{-10}	Han,2003
222	$\text{IO} + \text{O}(\text{^3P}) \rightarrow \text{I}(\text{^2P}_{3/2}) + \text{O}_2(\text{a}^1\Delta)$	1.5×10^{-11}	Han,2003
223	$2 \text{IO} \rightarrow \text{O}_2(\text{^3X}) + 2 \text{I}(\text{^2P}_{3/2})$	8.21×10^{-11}	Han,2003
224	$\text{NO} + \text{NO}(\nu > \theta) + \text{O}_2(\text{^3X}) \rightarrow 2 \text{NO}_2$	$3.3 \times 10^{-39} \exp(530/\text{T})$	IUPAC, 2010
225	$\text{NO} + \text{O}(\text{^3P}) \rightarrow \text{NO}_2^*$	2.49×10^{-17}	Kaufman,1958
226	$\text{NO} + \text{O}(\text{^3P}) + \text{O}_2(\text{^3X}) \rightarrow \text{NO}_2 + \text{O}_2(\text{^3X})$	$4.68 \times 10^{-28} \text{ T}^{-1.5}$	Atkinson,1997
227	$\text{NO} + \text{O}_2(\text{b}^1\Sigma) \rightarrow \text{NO} + \text{O}_2(\text{a}^1\Delta)$	6×10^{-14}	Atkinson,1997
228	$\text{NO} + \text{O}_3 \rightarrow \text{NO}_2 + \text{O}_2(\text{^3X})$	$1.79 \times 10^{-12} \exp(1370/\text{T})$	Atkinson,1997
229	$\text{NO}_2 + \text{O}(\text{^3P}) \rightarrow \text{NO} + \text{O}_2(\text{^3X})$	$6.64 \times 10^{-12} \exp(120/\text{T})$	Atkinson,1997
230	$\text{NO}_2 + \text{O}(\text{^3P}) \rightarrow \text{NO} + \text{O}_2(\text{a}^1\Delta)$	$0 \exp(120/\text{T})$	Atkinson,1997
231	$\text{NO}_2 + \text{O}_2(\text{b}^1\Sigma) \rightarrow \text{NO}_2 + \text{O}_2(\text{a}^1\Delta)$	4.1×10^{-13}	Atkinson,1997
232	$\text{NO}_2^* \rightarrow \text{NO}_2$	3.33×10^4	Kaufman, 1958
233	$\text{NO}(\nu > \theta) + \text{O}_3 \rightarrow \text{NO}_2 + \text{O}_2(\text{^3X})$	$1.79 \times 10^{-12} \exp(1370/\text{T})$	Atkinson,1997
234	$\text{O}(\text{^3P}) + \text{O}^+ + \text{O}_2(\text{^3X}) \rightarrow \text{O}_2(\text{^3X}) + \text{O}_2^+$	$5.77 \times 10^{-31} \text{ T}^{0.5}$	Gordiets,1995
235	$\text{O}(\text{^3P}) + \text{O}^- \rightarrow \text{O}_2(\text{^3X}) + e^-$	$1.15 \times 10^{-11} \text{ T}^{0.5}$	Ikezoe, 1986
236	$\text{O}(\text{^3P}) + \text{O}(\text{^1D}) \rightarrow 2 \text{O}(\text{^3P})$	7.99×10^{-12}	Gordiets,1995
237	$\text{O}(\text{^3P}) + \text{O}(\text{^1S}) \rightarrow \text{O}(\text{^3P}) + \text{O}(\text{^1D})$	$1.66 \times 10^{-11} \exp(-300/\text{T})$	Herron,2001
238	$\text{O}(\text{^3P}) + \text{O}(\text{^1S}) \rightarrow 2 \text{O}(\text{^3P})$	$3.33 \times 10^{-11} \exp(-300/\text{T})$	Herron,2001
239	$\text{O}(\text{^3P}) + \text{O}_2(\text{^3X}) + \text{O}_2(\text{a}^1\Delta) \rightarrow \text{O}(\text{^3P}) + 2 \text{O}_2(\text{^3X})$	1×10^{-32}	Vasiljeva,2004
240	$\text{O}(\text{^3P}) + \text{O}_2(\text{^3X}) + \text{O}_2(\text{a}^1\Delta) \rightarrow \text{O}_2(\text{a}^1\Delta) + \text{O}_3$	$5.19 \times 10^{-27} \text{ T}^{-2.8}$	Atkinson,1997
241	$\text{O}(\text{^3P}) + \text{O}_2(\text{^3X}) + \text{Xe} \rightarrow \text{O}_3 + \text{Xe}$	$5.19 \times 10^{-27} \text{ T}^{-2.8}$	†
242	$\text{O}(\text{^3P}) + 2 \text{O}_2(\text{^3X}) \rightarrow \text{O}_2(\text{^3X}) + \text{O}_3$	$5.19 \times 10^{-27} \text{ T}^{-2.8}$	Atkinson,1997
243	$\text{O}(\text{^3P}) + \text{O}_2^- \rightarrow \text{O}^- + \text{O}_2(\text{^3X})$	$8.66 \times 10^{-12} \text{ T}^{0.5}$	Ikezoe, 1986
244	$\text{O}(\text{^3P}) + \text{O}_2^- \rightarrow \text{O}_3 + e^-$	$8.66 \times 10^{-12} \text{ T}^{0.5}$	Ikezoe, 1986
245	$\text{O}(\text{^3P}) + \text{O}_2(\text{a}^1\Delta) \rightarrow \text{O}(\text{^3P}) + \text{O}_2(\text{^3X})$	1.99×10^{-16}	Herron,2001
246	$\text{O}(\text{^3P}) + \text{O}_2(\text{b}^1\Sigma) \rightarrow \text{O}(\text{^3P}) + \text{O}_2(\text{^3X})$	8.01×10^{-15}	Atkinson,1997
247	$\text{O}(\text{^3P}) + \text{O}_2(\text{b}^1\Sigma) \rightarrow \text{O}(\text{^3P}) + \text{O}_2(\text{a}^1\Delta)$	7.21×10^{-14}	Atkinson,1997
248	$\text{O}(\text{^3P}) + \text{O}_2(\text{^3X}, \nu = l) \rightarrow \text{O}(\text{^3P}) + \text{O}_2(\text{^3X})$	$5.77 \times 10^{-16} \text{ T}^{0.5}$	‡
249	$\text{O}(\text{^3P}) + \text{O}_3 \rightarrow 2 \text{O}_2(\text{^3X})$	$8.01 \times 10^{-12} \exp(-2060/\text{T})$	Atkinson,1997
250	$\text{O}(\text{^3P}) + \text{O}_3^- \rightarrow \text{O}_2(\text{^3X}) + \text{O}_2^-$	$1.44 \times 10^{-11} \text{ T}^{0.5}$	Ikezoe, 1986
251	$3 \text{O}(\text{^3P}) \rightarrow \text{O}(\text{^3P}) + \text{O}_2(\text{^3X})$	$4.5 \times 10^{-34} \exp(630/\text{T})$	Herron,2001
252	$3 \text{O}(\text{^3P}) \rightarrow \text{O}(\text{^3P}) + \text{O}_2(\text{a}^1\Delta)$	$2.51 \times 10^{-33} \text{ T}^{-0.63}$	Gordiets,1995
253	$\text{O}^+ + \text{O}^- \rightarrow 2 \text{O}(\text{^3P})$	$6 \times 10^{-5} \text{ T}^{-1}$	Gordiets,1995
254	$\text{O}^+ + \text{O}^- + \text{O}_2(\text{^3X}) \rightarrow \text{O}_2(\text{^3X}) + 2 \text{O}(\text{^3P})$	$3.11 \times 10^{-19} \text{ T}^{-2.5}$	Gordiets,1995

255	$O^+ + O_2(^3X) \rightarrow O(^3P) + O_2^+$	$1.95 \times 10^{-10} T^{0.4}$	Ikezoe, 1986
256	$O^+ + O_2^- \rightarrow O(^3P) + O_2(^3X)$	$6 \times 10^{-5} T^{-1}$	Gordiets, 1995
257	$O^+ + O_3 \rightarrow O_2(^3X) + O_2^+$	1×10^{-10}	Gordiets, 1995
258	$O^+ + O_3^- \rightarrow O(^3P) + O_3$	$6 \times 10^{-5} T^{-1}$	Gordiets, 1995
259	$O^- + O_2(^3X) \rightarrow O_3 + e^-$	$2.88 \times 10^{-16} T^{0.5}$	Gordiets, 1995
260	$O^- + O_2(^3X) + O_2^+ \rightarrow O(^3P) + 2 O_2(^3X)$	$3.11 \times 10^{-19} T^{-2.5}$	Gordiets, 1995
261	$O^- + O_2^+ \rightarrow O(^3P) + O_2(^3X)$	$6 \times 10^{-5} T^{-1}$	Gordiets, 1995
262	$O^- + O_2^+ \rightarrow 3 O(^3P)$	1×10^{-7}	Gordiets, 1995
263	$O^- + O_2(a^1\Delta) \rightarrow O_3 + e^-$	$1.73 \times 10^{-11} T^{0.5}$	Ikezoe, 1986
264	$O^- + O_2(b^1\Sigma) \rightarrow O(^3P) + O_2(^3X) + e^-$	$3.98 \times 10^{-11} T^{0.5}$	Gordiets, 1995
265	$O^- + O_3 \rightarrow O(^3P) + O_3^-$	$1.14 \times 10^{-11} T^{0.5}$	Ikezoe, 1986
266	$O^- + O_3 \rightarrow O_2(^3X) + O_2^-$	$5.88 \times 10^{-13} T^{0.5}$	Ikezoe, 1986
267	$O^- + O_3 \rightarrow 2 O_2(^3X) + e^-$	$1.73 \times 10^{-11} T^{0.5}$	Ikezoe, 1986
268	$O(^1D) + O_2(^3X) \rightarrow O(^3P) + O_2(^3X)$	$4.8 \times 10^{-12} \exp(67/T)$	Atkinson, 1997
269	$O(^1D) + O_2(^3X) \rightarrow O(^3P) + O_2(a^1\Delta)$	$1.59 \times 10^{-12} \exp(67/T)$	Atkinson, 1997
270	$O(^1D) + O_2(^3X) \rightarrow O(^3P) + O_2(b^1\Sigma)$	$2.55 \times 10^{-11} \exp(67/T)$	Atkinson, 1997
271	$O(^1D) + O_2(^3X) + O_2(a^1\Delta) \rightarrow O_2(a^1\Delta) + O_3$	$5.19 \times 10^{-27} T^{-2.8}$	†
272	$O(^1D) + 2 O_2(^3X) \rightarrow O_2(^3X) + O_3$	$5.19 \times 10^{-27} T^{-2.8}$	†
273	$O(^1D) + O_3 \rightarrow O_2(^3X) + 2 O(^3P)$	1.2×10^{-10}	Atkinson, 1997
274	$O(^1D) + O_3 \rightarrow 2 O_2(^3X)$	1.2×10^{-10}	Atkinson, 1997
275	$O(^1S) + O_2(^3X) \rightarrow O(^3P) + O_2(^3X)$	$1.59 \times 10^{-12} \exp(-850/T)$	Herron, 2001
276	$O(^1S) + O_2(^3X) \rightarrow O(^1D) + O_2(^3X)$	$3.19 \times 10^{-12} \exp(-850/T)$	Herron, 2001
277	$O(^1S) + O_2(a^1\Delta) \rightarrow O(^3P) + O_2(^3X)$	1.09×10^{-10}	Gordiets, 1995
278	$O(^1S) + O_2(a^1\Delta) \rightarrow 3 O(^3P)$	3.19×10^{-11}	Gordiets, 1995
279	$O(^1S) + O_2(a^1\Delta) \rightarrow O(^1D) + O_2(b^1\Sigma)$	2.89×10^{-11}	Gordiets, 1995
280	$O(^1S) + O_3 \rightarrow 2 O_2(^3X)$	5.79×10^{-10}	Herron, 2001
281	$O_2(^3X) + 2 NO \rightarrow 2 NO_2$	$3.3 \times 10^{-39} \exp(530/T)$	IUPAC, 2010
282	$O_2(^3X) + 2 NO(\nu > 0) \rightarrow 2 NO_2$	$3.3 \times 10^{-39} \exp(530/T)$	†
283	$O_2(^3X) + 2 O(^3P) \rightarrow O(^3P) + O_3$	$5.19 \times 10^{-27} T^{-2.800}$	Atkinson, 1997
284	$O_2(^3X) + 2 O(^3P) \rightarrow O_2(^3X) + O_2(a^1\Delta)$	$7.01 \times 10^{-34} T^{-0.63}$	Gordiets, 1995
285	$O_2(^3X) + 2 O(^3P) \rightarrow 2 O_2(^3X)$	$4.5 \times 10^{-34} \exp(630/T)$	Herron, 2001
286	$O_2(^3X) + O_2^+ \rightarrow O_2(^3X) + O_2^+$	$5.77 \times 10^{-11} T^{0.5}$	Stafford, 2004
287	$O_2(^3X) + O_2(a^1\Delta) \rightarrow O(^3P) + O_3$	$1.7 \times 10^{-22} T^{0.5}$	Stafford, 2004
288	$O_2(^3X) + O_3 \rightarrow O(^3P) + 2 O_2(^3X)$	$1.56 \times 10^{-9} \exp(-11490/T)$	Stafford, 2004
289	$O_2^+ + O_2^- \rightarrow O_2(^3X) + 2 O(^3P)$	1×10^{-7}	Gordiets, 1995
290	$O_2^+ + O_2^- \rightarrow 2 O_2(^3X)$	$6 \times 10^{-5} T^{-1}$	Gordiets, 1995
291	$O_2^+ + O_3^- \rightarrow O_2(^3X) + O_3$	$6 \times 10^{-5} T^{-1}$	Gordiets, 1995
292	$O_2^+ + O_3^- \rightarrow O_3 + 2 O(^3P)$	1×10^{-7}	Gordiets, 1995
293	$O_2^- + O_2(a^1\Delta) \rightarrow 2 O_2(^3X) + e^-$	$1.15 \times 10^{-11} T^{0.5}$	Ikezoe, 1986
294	$O_2^- + O_3 \rightarrow O_2(^3X) + O_3^-$	$3.46 \times 10^{-11} T^{0.5}$	Ikezoe, 1986
295	$O_2(a^1\Delta) + 2 O(^3P) \rightarrow O_2(^3X) + O_2(a^1\Delta)$	$4.5 \times 10^{-34} \exp(630/T)$	Herron, 2001
296	$O_2(a^1\Delta) + O_3 \rightarrow O(^3P) + 2 O_2(^3X)$	$5.2 \times 10^{-11} \exp(-2840/T)$	Atkinson, 1997
297	$O_2(b^1\Sigma) + O_3 \rightarrow O(^3P) + 2 O_2(^3X)$	1.53×10^{-11}	Atkinson, 1997
298	$O_2(b^1\Sigma) + O_3 \rightarrow O_2(^3X) + O_3$	3.3×10^{-12}	Atkinson, 1997
299	$O_2(b^1\Sigma) + O_3 \rightarrow O_2(a^1\Delta) + O_3$	3.3×10^{-12}	Atkinson, 1997
300	$O(3p^3P) \rightarrow O(^3P)$	3.69×10^7	Ralchencko, 2008
301	$O(3p^5P) \rightarrow O(^3P)$	3.22×10^7	Ralchencko, 2008
302	$Xe + 2 O(^3P) \rightarrow O_2(^3X) + Xe$	$4.5 \times 10^{-34} \exp(630/T)$	†
303	$Ar + e^- \leftrightarrow Ar^* + e^-$	$f(EED)$	Phelps, 1985
305	$Ar + e^- \rightarrow Ar^+ + 2 e^-$	$f(EED)$	Phelps, 1985

306	$\text{Ar} + e^- \leftrightarrow \text{Ar}(2p^1) + e^-$	$f(EED)$	Phelps,1985
308	$\text{Ar} + e^- \leftrightarrow \text{Ar}(2p^5) + e^-$	$f(EED)$	Phelps,1985
310	$\text{Ar} + e^- \leftrightarrow \text{Ar}(2p^7) + e^-$	$f(EED)$	Phelps,1985
312	$\text{Ar} + e^- \leftrightarrow \text{Ar}(2p^9) + e^-$	$f(EED)$	Phelps,1985
314	$\text{Ar}^* + e^- \rightarrow \text{Ar}^+ + 2 e^-$	$f(EED)$	Phelps,1985
315	$\text{He} + e^- \leftrightarrow \text{He}^* + e^-$	$f(EED)$	Boeuf, 1982
317	$\text{He} + e^- \rightarrow \text{He}^+ + 2 e^-$	$f(EED)$	Rapp,1965
318	$\text{He} + \text{O}_2(^3X) + e^- \rightarrow \text{He} + \text{O}_2^-$	$f(EED)$	‡
319	$\text{He}^* + e^- \rightarrow \text{He}^+ + 2 e^-$	$f(EED)$	Vriens,1964
320	$\text{NO} + e^- \rightarrow \text{NO}^+ + 2 e^-$	$f(EED)$	Phelps,1985
321	$\text{NO} + e^- \leftrightarrow \text{NO}(v>0) + e^-$	$f(EED)$	Phelps,1985
323	$\text{NO} + e^- \leftrightarrow \text{NO}(v>0) + e^-$	$f(EED)$	Phelps,1985
325	$\text{NO} + e^- \leftrightarrow \text{NO}(v>0) + e^-$	$f(EED)$	Phelps,1985
327	$\text{NO} + e^- \leftrightarrow \text{NO}(v>0) + e^-$	$f(EED)$	Phelps,1985
329	$\text{NO} + e^- \leftrightarrow \text{NO}(v>0) + e^-$	$f(EED)$	Phelps,1985
331	$\text{NO} + e^- \leftrightarrow \text{NO}(v>0) + e^-$	$f(EED)$	Phelps,1985
333	$\text{NO}_2 + e^- \rightarrow \text{NO} + \text{O}^+ + 2 e^-$	$f(EED)$	‡
334	$\text{NO}_2 + e^- \rightarrow \text{NO}^+ + \text{O}(^3P) + 2 e^-$	$f(EED)$	‡
335	$\text{NO}_2 + e^- \rightarrow \text{NO}_2^+ + 2 e^-$	$f(EED)$	‡
336	$\text{O}(^3P) + e^- \rightarrow \text{O}^+ + 2 e^-$	$f(EED)$	Laher,1990
337	$\text{O}(^3P) + e^- \leftrightarrow \text{O}(^1D) + e^-$	$f(EED)$	Laher,1990
339	$\text{O}(^3P) + e^- \leftrightarrow \text{O}(^1S) + e^-$	$f(EED)$	Laher,1990
341	$\text{O}(^3P) + e^- \leftrightarrow \text{O}(3p^3P) + e^-$	$f(EED)$	‡
343	$\text{O}(^3P) + e^- \leftrightarrow \text{O}(3p^5P) + e^-$	$f(EED)$	‡
345	$\text{O}^+ + e^- \rightarrow \text{O}(^3P)$	$f(EED)$	‡
346	$\text{O}^+ + e^- \rightarrow \text{O}(^1D)$	$f(EED)$	‡
347	$\text{O}^- + e^- \rightarrow \text{O}(^3P) + 2 e^-$	$f(EED)$	‡
348	$\text{O}(^1D) + e^- \rightarrow \text{O}^+ + 2 e^-$	$f(EED)$	†
349	$\text{O}(^1S) + e^- \rightarrow \text{O}^+ + 2 e^-$	$f(EED)$	†
350	$\text{O}_2(^3X) + e^- \rightarrow \text{O}(^3P) + \text{O}^+ + 2 e^-$	$f(EED)$	Phelps,1985
351	$\text{O}_2(^3X) + e^- \rightarrow \text{O}(^3P) + \text{O}^-$	$f(EED)$	Phelps,1985
352	$\text{O}_2(^3X) + e^- \rightarrow \text{O}(^3P) + \text{O}(^1D) + e^-$	$f(EED)$	Phelps,1985
353	$\text{O}_2(^3X) + e^- \rightarrow 2 \text{O}(^3P) + e^-$	$f(EED)$	Phelps,1985
354	$\text{O}_2(^3X) + e^- \rightarrow \text{O}_2^+ + 2 e^-$	$f(EED)$	Phelps,1985
355	$\text{O}_2(^3X) + e^- \leftrightarrow \text{O}_2(a^1\Delta) + e^-$	$f(EED)$	Phelps,1985
357	$\text{O}_2(^3X) + e^- \leftrightarrow \text{O}_2(b^1\Sigma) + e^-$	$f(EED)$	Phelps,1985
359	$\text{O}_2(^3X) + e^- \leftrightarrow \text{O}_2(^3X, v=1) + e^-$	$f(EED)$	Phelps,1985
361	$\text{O}_2(^3X) + e^- \leftrightarrow \text{O}_2(^3X, v=2) + e^-$	$f(EED)$	Phelps,1985
363	$\text{O}_2(^3X) + e^- \leftrightarrow \text{O}_2(^3X, v=3) + e^-$	$f(EED)$	Phelps,1985
365	$\text{O}_2(^3X) + e^- \leftrightarrow \text{O}_2(^3X, v=4) + e^-$	$f(EED)$	Phelps,1985
367	$\text{O}_2^+ + e^- \rightarrow \text{O}(^3P) + \text{O}(^1D)$	$f(EED)$	Phelps,1985
368	$\text{O}_2^+ + e^- \rightarrow 2 \text{O}(^3P)$	$f(EED)$	Phelps,1985
369	$\text{O}_2(a^1\Delta) + e^- \rightarrow \text{O}(^3P) + \text{O}^+ + 2 e^-$	$f(EED)$	†
370	$\text{O}_2(a^1\Delta) + e^- \rightarrow \text{O}(^3P) + \text{O}^-$	$f(EED)$	Burrow,1973
371	$\text{O}_2(a^1\Delta) + e^- \rightarrow \text{O}(^3P) + \text{O}(^1D) + e^-$	$f(EED)$	†
372	$\text{O}_2(a^1\Delta) + e^- \rightarrow 2 \text{O}(^3P) + e^-$	$f(EED)$	†
373	$\text{O}_2(a^1\Delta) + e^- \rightarrow 2 \text{O}(^1D) + e^-$	$f(EED)$	†
374	$\text{O}_2(a^1\Delta) + e^- \rightarrow \text{O}_2^+ + 2 e^-$	$f(EED)$	†
375	$\text{O}_2(a^1\Delta) + e^- \leftrightarrow \text{O}_2(b^1\Sigma) + e^-$	$f(EED)$	Hall,1975
377	$\text{O}_2(b^1\Sigma) + e^- \rightarrow \text{O}(^3P) + \text{O}^+ + 2 e^-$	$f(EED)$	†

378	$O_2(b^1\Sigma) + e^- \rightarrow O(^3P) + O^-$	$f(EED)$	†
379	$O_2(b^1\Sigma) + e^- \rightarrow O(^3P) + O(^1D) + e^-$	$f(EED)$	†
380	$O_2(b^1\Sigma) + e^- \rightarrow 2 O(^3P) + e^-$	$f(EED)$	†
381	$O_2(b^1\Sigma) + e^- \rightarrow 2 O(^1D) + e^-$	$f(EED)$	†
382	$O_2(b^1\Sigma) + e^- \rightarrow O_2^+ + 2 e^-$	$f(EED)$	†
383	$O_2(^3X, v=1) + e^- \rightarrow O(^3P) + O^+ + 2 e^-$	$f(EED)$	†
384	$O_2(^3X, v=1) + e^- \rightarrow O(^3P) + O^-$	$f(EED)$	†
385	$O_2(^3X, v=1) + e^- \rightarrow O(^3P) + O(^1D) + e^-$	$f(EED)$	†
386	$O_2(^3X, v=1) + e^- \rightarrow 2 O(^3P) + e^-$	$f(EED)$	†
387	$O_2(^3X, v=1) + e^- \rightarrow 2 O(^1D) + e^-$	$f(EED)$	†
388	$O_2(^3X, v=1) + e^- \rightarrow O_2^+ + 2 e^-$	$f(EED)$	†
389	$O_2(^3X, v=1) + e^- \leftrightarrow O_2(a^1\Delta) + e^-$	$f(EED)$	†
391	$O_2(^3X, v=1) + e^- \leftrightarrow O_2(b^1\Sigma) + e^-$	$f(EED)$	†
393	$O_3 + e^- \rightarrow O(^3P) + O_2^-$	$f(EED)$	Matejcik,1997
394	$O_3 + e^- \rightarrow O^- + O_2(^3X)$	$f(EED)$	Matejcik,1997
395	$O(^3P) \rightarrow 1/2 O_2(^3X)$	$f(diffusion\ to\ wall)$	‡
396	$He + N_2(A^3\Sigma, v=0 \rightarrow 4) \rightarrow He + N_2$	5.4×10^{-12}	†
397	$N + NO \rightarrow N_2 + O(^3P)$	$1.6 \times 10^{-10} \exp(-459.0/T)$	Fisher,1997
398	$N + NO \rightarrow N_2 + O(^3P)$	$4.98 \times 10^{-11} \exp(-99.0/T)$	Fisher,1997
399	$N + NO_2 \rightarrow N_2 + O_2(^3X)$	$5.79 \times 10^{-12} \exp(220.0/T)$	Wennberg,1994
400	$N + NO_2 \rightarrow N_2O + O(^3P)$	$5.79 \times 10^{-12} \exp(220.0/T)$	Wennberg,1994
401	$N + O(^3P) + M \rightarrow NO + M$	$5.45 \times 10^{-33} \exp(155.0/T)$	Campbell,1973
402	$N + O_2(^3X) \rightarrow NO + O(^3P)$	$3.82 \times 10^{-12} \exp(-2981.0/T)$	Mavroyannis,1961
403	$N + O_2(a^1\Delta) \rightarrow NO + O(^3P)$	9×10^{-17}	Demore,1997
404	$N + O_3 \rightarrow NO + O_2(^3X)$	2×10^{-16}	Demore,1997
405	$2 N + M \rightarrow N_2 + M$	$8.3 \times 10^{-34} \exp(2356.0/T)$	Forst,1957
406	$N_2 + N_2(A^3\Sigma, v=0 \rightarrow 4) \rightarrow 2 N_2$	3×10^{-18}	Herron,1999
407	$N_2 + O(^3P) \rightarrow N + NO$	$4.23 \times 10^{-11} T^{0.151} \exp(-37457.0/T)$	Fisher,1997
408	$N_2 + O(^1D) \rightarrow N_2 + O(^3P)$	$1.79 \times 10^{-11} \exp(109.0/T)$	Demore,1997
409	$N_2 + O(^1D) + M \rightarrow N_2 + O(^3P) + M$	$4.23 \times 10^{-34} T^{0.88}$	Estupinan,2002
410	$N_2(A^3\Sigma, v=0 \rightarrow 4) + O(^3P) \rightarrow N_2 + O(^3P)$	4.6×10^{-11}	Herron,1999
411	$N_2(A^3\Sigma, v=0 \rightarrow 4) + O_2(^3X) \rightarrow N_2 + O_2(^3X)$	5.4×10^{-12}	Herron,1999
412	$N_2(A^3\Sigma, v=0 \rightarrow 4) + O_2(a^1\Delta) \rightarrow N_2 + 2 O(^3P)$	1.99×10^{-11}	Herron,1999
413	$N_2O + M \rightarrow N_2 + O(^3P) + M$	$2.49 \times 10^{-11} \exp(-16236.0/T)$	Lesar,1993
414	$N_2O + NO \rightarrow N_2 + NO_2$	$8.71 \times 10^{-19} T^{2.23} \exp(-23332.0/T)$	Mebel,1996
415	$N_2O + O(^3P) \rightarrow N_2 + O_2(^3X)$	$6.13 \times 10^{-12} \exp(-8019.0/T)$	Meagher,2000
416	$N_2O + O(^3P) \rightarrow 2 NO$	$1.49 \times 10^{-10} \exp(-14071.0/T)$	Zuev,1991
417	$N_2O + O(^1D) \rightarrow N_2 + O_2(^3X)$	4.39×10^{-11}	Atkinson,1977
418	$N_2O + O(^1D) \rightarrow N_2 + O_2(a^1\Delta)$	$4.94 \times 10^{-18} T^{2.300} \exp(-1159.0/T)$	Gonzalez,2002
419	$N_2O + O(^1D) \rightarrow N_2O + O(^3P)$	9.99×10^{-13}	Atkinson,1977
420	$N_2O + O(^1D) \rightarrow 2 NO$	7.21×10^{-11}	Atkinson,1977
421	$N_2O + O_2(a^1\Delta) \rightarrow N_2O + O_2(^3X)$	5×10^{-20}	Findlay,1971
422	$N_2(v=1) + O(^3P) \rightarrow N + NO$	$4.47 \times 10^{-11} T^{0.145} \exp(-35776.0/T)$	Fisher,1997
423	$N_2(v=2) + O(^3P) \rightarrow N + NO$	$4.47 \times 10^{-11} T^{0.147} \exp(-34077.0/T)$	Fisher,1997
424	$N_2(v=3) + O(^3P) \rightarrow N + NO$	$4.4 \times 10^{-11} T^{0.146} \exp(-32385.0/T)$	Fisher,1997
425	$N_2(v=4) + O(^3P) \rightarrow N + NO$	$4.44 \times 10^{-11} T^{0.151} \exp(-30679.0/T)$	Fisher,1997
426	$N_2(v=5) + O(^3P) \rightarrow N + NO$	$4.25 \times 10^{-11} T^{0.141} \exp(-29008.0/T)$	Fisher,1997
427	$N_2(v=6) + O(^3P) \rightarrow N + NO$	$4.65 \times 10^{-11} T^{0.143} \exp(-27308.0/T)$	Fisher,1997
428	$N_2(v=7) + O(^3P) \rightarrow N + NO$	$4.57 \times 10^{-11} T^{0.146} \exp(-25609.0/T)$	Fisher,1997
429	$N_2(v=8) + O(^3P) \rightarrow N + NO$	$4.48 \times 10^{-11} T^{0.161} \exp(-23881.0/T)$	Fisher,1997

430	$N_2 + e^- \rightarrow 2 N + e^-$	$f(EED)$	Crosby,1993
431	$N_2 + e^- \leftrightarrow N_2(A^1\Pi) + e^-$	$f(EED)$	Phelps,1985
433	$N_2 + e^- \leftrightarrow N_2(A^1\Sigma) + e^-$	$f(EED)$	Phelps,1985
435	$N_2 + e^- \leftrightarrow N_2(A^3\Sigma, v=0 \rightarrow 4) + e^-$	$f(EED)$	Phelps,1985
437	$N_2 + e^- \leftrightarrow N_2(A^3\Sigma, v \geq 10) + e^-$	$f(EED)$	Phelps,1985
439	$N_2 + e^- \leftrightarrow N_2(A^3\Sigma, v=5 \rightarrow 9) + e^-$	$f(EED)$	Phelps,1985
441	$N_2 + e^- \leftrightarrow N_2(B^3\Pi) + e^-$	$f(EED)$	Phelps,1985
443	$N_2 + e^- \leftrightarrow N_2(A^1\Sigma) + e^-$	$f(EED)$	Phelps,1985
445	$N_2 + e^- \leftrightarrow N_2(v=1) + e^-$	$f(EED)$	Phelps,1985
447	$N_2 + e^- \leftrightarrow N_2(v=2) + e^-$	$f(EED)$	Phelps,1985
449	$N_2 + e^- \leftrightarrow N_2(v=3) + e^-$	$f(EED)$	Phelps,1985
451	$N_2 + e^- \leftrightarrow N_2(v=4) + e^-$	$f(EED)$	Phelps,1985
453	$N_2 + e^- \leftrightarrow N_2(v=5) + e^-$	$f(EED)$	Phelps,1985
455	$N_2 + e^- \leftrightarrow N_2(v=6) + e^-$	$f(EED)$	Phelps,1985
457	$N_2 + e^- \leftrightarrow N_2(v=7) + e^-$	$f(EED)$	Phelps,1985
459	$N_2 + e^- \leftrightarrow N_2(v=8) + e^-$	$f(EED)$	Phelps,1985
461	$N_2 + e^- \leftrightarrow N_2(W^3\Delta) + e^-$	$f(EED)$	Phelps,1985
463	$N_2(A^1\Pi) + e^- \rightarrow 2 N + e^-$	$f(EED)$	†
464	$N_2(A^1\Sigma) + e^- \rightarrow 2 N + e^-$	$f(EED)$	†
465	$N_2(A^3\Sigma, v=0 \rightarrow 4) + e^- \rightarrow 2 N + e^-$	$f(EED)$	†
466	$N_2(A^3\Sigma, v \geq 10) + e^- \rightarrow 2 N + e^-$	$f(EED)$	†
467	$N_2(A^3\Sigma, v=5 \rightarrow 9) + e^- \rightarrow 2 N + e^-$	$f(EED)$	†
468	$N_2(B^3\Pi) + e^- \rightarrow 2 N + e^-$	$f(EED)$	†
469	$N_2(A^1\Sigma) + e^- \rightarrow 2 N + e^-$	$f(EED)$	†
470	$N_2(v=1) + e^- \rightarrow 2 N + e^-$	$f(EED)$	†
471	$N_2(v=2) + e^- \rightarrow 2 N + e^-$	$f(EED)$	†
472	$N_2(v=3) + e^- \rightarrow 2 N + e^-$	$f(EED)$	†
473	$N_2(v=4) + e^- \rightarrow 2 N + e^-$	$f(EED)$	†
474	$N_2(v=5) + e^- \rightarrow 2 N + e^-$	$f(EED)$	†
475	$N_2(v=6) + e^- \rightarrow 2 N + e^-$	$f(EED)$	†
476	$N_2(v=7) + e^- \rightarrow 2 N + e^-$	$f(EED)$	†
477	$N_2(v=8) + e^- \rightarrow 2 N + e^-$	$f(EED)$	†
478	$N_2(W^3\Delta) + e^- \rightarrow 2 N + e^-$	$f(EED)$	†
479	$N_2(v=1) + M \leftrightarrow N_2 + M$	$5.64 \times 10^{-12} T^{0.939} \exp(-211.0/T^{1/3})$	Fisher,1997
481	$N_2(v=1) + N_2(v=2) \leftrightarrow N_2 + N_2(v=3)$	$6.08 \times 10^{-19} T^{1.764} \exp(193.0/T)$	Fisher,1997
483	$N_2(v=1) + N_2(v=3) \leftrightarrow N_2 + N_2(v=4)$	$8.11 \times 10^{-19} T^{1.764} \exp(193.0/T)$	Fisher,1997
485	$N_2(v=1) + N_2(v=4) \leftrightarrow N_2 + N_2(v=5)$	$1.01 \times 10^{-18} T^{1.764} \exp(193.0/T)$	Fisher,1997
487	$N_2(v=1) + N_2(v=5) \leftrightarrow N_2 + N_2(v=6)$	$1.21 \times 10^{-18} T^{1.764} \exp(193.0/T)$	Fisher,1997
489	$N_2(v=1) + N_2(v=6) \leftrightarrow N_2 + N_2(v=7)$	$1.42 \times 10^{-18} T^{1.764} \exp(193.0/T)$	Fisher,1997
491	$N_2(v=1) + N_2(v=7) \leftrightarrow N_2 + N_2(v=8)$	$1.62 \times 10^{-18} T^{1.764} \exp(193.0/T)$	Fisher,1997
493	$2 N_2(v=1) \leftrightarrow N_2 + N_2(v=2)$	$4.05 \times 10^{-19} T^{1.764} \exp(193.0/T)$	Fisher,1997
495	$N_2(v=2) + M \leftrightarrow N_2(v=1) + M$	$1.12 \times 10^{-11} T^{0.939} \exp(-211.0/T^{1/3})$	Fisher,1997
497	$N_2(v=2) + N_2(v=3) \leftrightarrow N_2(v=1) + N_2(v=4)$	$1.62 \times 10^{-18} T^{1.764} \exp(193.0/T)$	Fisher,1997
499	$N_2(v=2) + N_2(v=4) \leftrightarrow N_2(v=1) + N_2(v=5)$	$2.02 \times 10^{-18} T^{1.764} \exp(193.0/T)$	Fisher,1997
501	$N_2(v=2) + N_2(v=5) \leftrightarrow N_2(v=1) + N_2(v=6)$	$2.43 \times 10^{-18} T^{1.764} \exp(193.0/T)$	Fisher,1997
503	$N_2(v=2) + N_2(v=6) \leftrightarrow N_2(v=1) + N_2(v=7)$	$2.84 \times 10^{-18} T^{1.764} \exp(193.0/T)$	Fisher,1997
505	$N_2(v=2) + N_2(v=7) \leftrightarrow N_2(v=1) + N_2(v=8)$	$3.24 \times 10^{-18} T^{1.764} \exp(193.0/T)$	Fisher,1997
507	$2 N_2(v=2) \leftrightarrow N_2(v=1) + N_2(v=3)$	$1.21 \times 10^{-18} T^{1.764} \exp(193.0/T)$	Fisher,1997
509	$N_2(v=3) + M \leftrightarrow N_2(v=2) + M$	$1.69 \times 10^{-11} T^{0.939} \exp(-211.0/T^{1/3})$	Fisher,1997
511	$N_2(v=3) + N_2(v=4) \leftrightarrow N_2(v=2) + N_2(v=5)$	$3.04 \times 10^{-18} T^{1.764} \exp(193.0/T)$	Fisher,1997

513	$N_2(v=3) + N_2(v=5) \leftrightarrow N_2(v=2) + N_2(v=6)$	$3.65 \times 10^{-18} T^{1.764} \exp(193.0/T)$	Fisher,1997
515	$N_2(v=3) + N_2(v=6) \leftrightarrow N_2(v=2) + N_2(v=7)$	$4.26 \times 10^{-18} T^{1.764} \exp(193.0/T)$	Fisher,1997
517	$N_2(v=3) + N_2(v=7) \leftrightarrow N_2(v=2) + N_2(v=8)$	$4.87 \times 10^{-18} T^{1.764} \exp(193.0/T)$	Fisher,1997
519	$2 N_2(v=3) \leftrightarrow N_2(v=2) + N_2(v=4)$	$2.43 \times 10^{-18} T^{1.764} \exp(193.0/T)$	Fisher,1997
521	$N_2(v=4) + M \leftrightarrow N_2(v=3) + M$	$2.25 \times 10^{-11} T^{0.939} \exp(-211.0/T^{1/3})$	Fisher,1997
523	$N_2(v=4) + N_2(v=5) \leftrightarrow N_2(v=3) + N_2(v=6)$	$4.87 \times 10^{-18} T^{1.764} \exp(193.0/T)$	Fisher,1997
525	$N_2(v=4) + N_2(v=6) \leftrightarrow N_2(v=3) + N_2(v=7)$	$5.68 \times 10^{-18} T^{1.764} \exp(193.0/T)$	Fisher,1997
527	$N_2(v=4) + N_2(v=7) \leftrightarrow N_2(v=3) + N_2(v=8)$	$6.49 \times 10^{-18} T^{1.764} \exp(193.0/T)$	Fisher,1997
529	$2 N_2(v=4) \leftrightarrow N_2(v=3) + N_2(v=5)$	$4.05 \times 10^{-18} T^{1.764} \exp(193.0/T)$	Fisher,1997
531	$N_2(v=5) + M \leftrightarrow N_2(v=4) + M$	$2.82 \times 10^{-11} T^{0.939} \exp(-211.0/T^{1/3})$	Fisher,1997
533	$N_2(v=5) + N_2(v=6) \leftrightarrow N_2(v=4) + N_2(v=7)$	$7.1 \times 10^{-18} T^{1.764} \exp(193.0/T)$	Fisher,1997
535	$N_2(v=5) + N_2(v=7) \leftrightarrow N_2(v=4) + N_2(v=8)$	$8.11 \times 10^{-18} T^{1.764} \exp(193.0/T)$	Fisher,1997
537	$2 N_2(v=5) \leftrightarrow N_2(v=4) + N_2(v=6)$	$6.08 \times 10^{-18} T^{1.764} \exp(193.0/T)$	Fisher,1997
539	$N_2(v=6) + M \leftrightarrow N_2(v=5) + M$	$3.38 \times 10^{-11} T^{0.939} \exp(-211.0/T^{1/3})$	Fisher,1997
541	$N_2(v=6) + N_2(v=7) \leftrightarrow N_2(v=5) + N_2(v=8)$	$9.74 \times 10^{-18} T^{1.764} \exp(193.0/T)$	Fisher,1997
543	$2 N_2(v=6) \leftrightarrow N_2(v=5) + N_2(v=7)$	$8.52 \times 10^{-18} T^{1.764} \exp(193.0/T)$	Fisher,1997
545	$N_2(v=7) + M \leftrightarrow N_2(v=6) + M$	$3.95 \times 10^{-11} T^{0.939} \exp(-211.0/T^{1/3})$	Fisher,1997
547	$2 N_2(v=7) \leftrightarrow N_2(v=6) + N_2(v=8)$	$1.13 \times 10^{-17} T^{1.764} \exp(193.0/T)$	Fisher,1997
549	$N_2(v=8) + M \leftrightarrow N_2(v=7) + M$	$4.51 \times 10^{-11} T^{0.939} \exp(-211.0/T^{1/3})$	Fisher,1997